Eur. Phys. J. C (2017) 77:415
DOI 10.1140/epjc/s10052-017-4980-9

THE EUROPEAN PHYSICAL JOURNAL C

Regular Article - Theoretical Physics

Study of the weak annihilation contributions in charmless $B_s \to VV$ decays

Qin Chang[1,2], **Xiaonan Li**[1], **Xin-Qiang Li**[2,a], **Junfeng Sun**[1]

[1] Institute of Particle and Nuclear Physics, Henan Normal University, Henan 453007, China
[2] Institute of Particle Physics and Key Laboratory of Quark and Lepton Physics (MOE), Central China Normal University, Wuhan 430079, Hubei, China

Received: 23 March 2017 / Accepted: 8 June 2017 / Published online: 20 June 2017

Abstract In this paper, in order to probe the spectator-scattering and weak annihilation contributions in charmless $B_s \to VV$ (where V stands for a light vector meson) decays, we perform the χ^2-analyses for the endpoint parameters within the QCD factorization framework, under the constraints from the measured $\bar{B}_s \to \rho^0\phi$, ϕK^{*0}, $\phi\phi$ and $K^{*0}\bar{K}^{*0}$ decays. The fitted results indicate that the endpoint parameters in the factorizable and nonfactorizable annihilation topologies are non-universal, which is also favored by the charmless $B \to PP$ and PV (where P stands for a light pseudo-scalar meson) decays observed in previous work. Moreover, the abnormal polarization fractions $f_{L,\perp}(\bar{B}_s \to K^{*0}\bar{K}^{*0}) = (20.1\pm7.0)\%$, $(58.4\pm8.5)\%$ measured by the LHCb collaboration can be reconciled through the weak annihilation corrections. However, the branching ratio of $\bar{B}_s \to \phi K^{*0}$ decay exhibits a tension between the data and theoretical result, which dominates the contributions to $\chi^2_{\rm min}$ in the fits. Using the fitted endpoint parameters, we update the theoretical results for the charmless $B_s \to VV$ decays, which will be further tested by the LHCb and Belle-II experiments in the near future.

1 Introduction

Non-leptonic B-meson weak decays play an important role in testing the flavor dynamics of the standard model (SM) and exploring possible hints of new physics beyond it. Theoretically, one of the main obstacles for a reliable prediction on these decays is how to evaluate precisely the hadronic matrix elements of local operators between the initial and final hadronic states, especially due to the nontrivial QCD dynamics involved. To this end, several attractive QCD-inspired approaches, such as QCD factorization (QCDF) [1,2], perturbative QCD (pQCD) [3,4] and soft-collinear effective theory (SCET) [5–8], have been proposed in the last decades. However, the convolution integrals of the parton-level hard kernels with the asymptotic forms of light-cone distribution amplitudes (LCDAs) generally suffer from the endpoint divergence in the weak annihilation (WA) amplitudes. This divergence limits the predictive power and introduces large theoretical uncertainties.

In the QCDF approach, the endpoint divergent integrals, signaling of infrared-sensitive contributions, are usually parameterized by two complex quantities X_A and X_L that are defined, respectively, by [9,10]

$$\int_0^1 \frac{{\rm d}x}{x} \to X_A(\rho_A,\phi_A) = (1+\rho_A e^{i\phi_A})\ln\frac{m_b}{\Lambda_h}, \tag{1}$$

$$\int_0^1 \frac{{\rm d}x}{x^2} \to X_L(\rho_A,\phi_A) = (1+\rho_A e^{i\phi_A})\frac{m_b}{\Lambda_h}, \tag{2}$$

where $\Lambda_h = 0.5\,{\rm GeV}$, and the two phenomenological parameters ρ_A and ϕ_A account for the strength and possible strong phase of WA contributions near the endpoint, respectively. In addition, the spectator-scattering amplitudes also involve the endpoint divergence, which is dealt with the same manner by introducing the complex quantity $X_H(\rho_H,\phi_H) = X_A(\rho_A,\phi_A)|_{A\to H}$. The numerical values of $\rho_{A,H}$ and $\phi_{A,H}$ are unknown and can only be inferred by fitting them to the experimental data so far. While weakening the predictive power of the QCDF approach, the parameterization scheme provides a feasible way to explore the WA effects from a phenomenological point of view.

Theoretically, the WA contributions with possible strong phase have attracted a lot of attention in the past few years, for instance, in Refs. [11–30]. Traditionally, both ρ_A and ϕ_A are treated as universal parameters for different kinds of annihilation topologies. However, a global fit for the endpoint parameters indicates that, while a relatively large endpoint parameter is needed for the decays related by isospin sym-

[a] e-mail: xqli@itp.ac.cn

metry, there exist some tensions in $B \to \phi K^*$ and $B \to \pi K$ decays [22], with the latter exhibiting the so-called "πK CP-asymmetry puzzle".[1] In Refs. [23,24], after studying carefully the flavor dependence of the endpoint parameters in charmless $B \to PP$ (where P stands for a light pseudoscalar meson) decays, the authors suggest that the endpoint parameters should be topology-dependent. Such a topology-dependent parameterization scheme is also favored by most of the charmless $B \to PP$ and PV (where V stands for a light vector meson) decays, as demonstrated in Refs. [26–28], and it could provide a possible solution to the well-known "πK CP-asymmetry puzzle" [25]. In addition, using the recent measurements of the pure annihilation $B_s \to \pi^+\pi^-$ and $B_d \to K^+K^-$ decays by the CDF [36], Belle [37] and LHCb collaborations [38,39], the authors of Refs. [23,24] find significant flavor-symmetry breaking effects in the non-factorizable annihilation contributions.

Experimentally, due to the rapid development of dedicated heavy-flavor experiments, more precise measurements of non-leptonic B decays will be available. As reported in Ref. [40], for instance, over 10^{11} $b\bar{b}$ quark pairs are produced per fb^{-1} of data at the LHCb experiment. Furthermore, after the high-luminosity upgrade, a dataset of 50 fb^{-1} will be accumulated [41–44]. In addition, most recently, the SuperKEKB/Belle-II experiment has started test operations and succeeded in circulating and storing beams in the electron and positron rings. The annual integrated luminosity is expected to reach up to 13 ab^{-1}, and over 10^{10} samples of $b\bar{b}$ quark pairs will be accumulated by the Belle-II experiment [45]. Thus, the forthcoming measurements of not only $B_{u,d}$ but also B_s decays are expected to reach a high accuracy, which could provide us with a clearer picture of the WA contributions in these decays.

In this paper, motivated by the recent theoretical studies and the bright experimental prospects, we will investigate the WA contributions in charmless $B_s \to VV$ decays, which involve more observables than in charmless $B \to PP$ and PV decays and may provide much stronger constraints on the endpoint parameters. In addition, using the obtained values of the endpoint parameters, we will update the theoretical results for charmless $B_s \to VV$ decays within the QCDF framework.

Our paper is organized as follows. In Sect. 2, we review briefly the WA amplitudes within the QCDF framework and observables for charmless $B_s \to VV$ decays. Section 3 is devoted to the numerical results and discussions. Finally, we give our conclusion in Sect. 4.

[1] The direct CP-asymmetries $A_{\rm CP}^{\pi^0 K^+}$ in $B^\pm \to \pi^0 K^\pm$ and $A_{\rm CP}^{\pi^- K^+}$ in $B^0(\bar{B}^0) \to \pi^\mp K^\pm$ decays are expected to be roughly the same [31–33]. However, the current experimental data show a significant difference between them, $A_{\rm CP}^{\pi^0 K^+} - A_{\rm CP}^{\pi^- K^+} = 0.122 \pm 0.022$ [34,35], deviating from zero at about 5.6 σ level.

2 Brief review of the theoretical framework for charmless $B_s \to VV$ decays

2.1 Amplitudes in QCD factorization

In the SM, the effective weak Hamiltonian for non-leptonic B-meson decays is given by [46,47]

$$\begin{aligned}\mathcal{H}_{\rm eff} = \frac{G_F}{\sqrt{2}} \Big\{ & V_{ub}V_{up}^* \left(C_1 O_1^u + C_2 O_2^u\right) \\ & + V_{cb}V_{cp}^* \left(C_1 O_1^c + C_2 O_2^c\right) \\ & - V_{tb}V_{tp}^* \Big(\sum_{i=3}^{10} C_i O_i + C_{7\gamma} O_{7\gamma} + C_{8g} O_{8g} \Big) \Big\} + \text{h.c.},\end{aligned} \tag{3}$$

where $V_{qb}V_{qp}^*$, with $q \in \{u, c, t\}$ and $p \in \{d, s\}$, are products of the Cabibbo–Kobayashi–Maskawa (CKM) matrix elements, and C_i the Wilson coefficients of the effective operators O_i. Starting with the effective Hamiltonian and following the strategy proposed in Ref. [48], Beneke et al. proposed the QCDF approach to evaluate the hadronic matrix elements [1,2], which is now being widely used to analyze the B-meson weak decays (see, for instance, Refs. [9,31,49–55]). The theoretical framework for charmless $B \to VV$ decays has also been fully developed (cf. Refs. [19,20,53] for details). In this paper, we follow the same conventions as in Refs. [53,56].

Within the QCDF framework, after performing the convolution integrals of the $\mathcal{O}(\alpha_s)$ hard kernels with the asymptotic forms of the light-meson LCDAs, one gets the following basic building blocks of the WA amplitudes in charmless $B \to VV$ decays [53,56]:

$$A_1^{i,0} \simeq A_2^{i,0} \simeq 18\pi\alpha_s \left[\left(X_A^i - 4 + \frac{\pi^2}{3} \right) + r_\chi^{V_1} r_\chi^{V_2} \left(X_A^i - 2 \right)^2 \right], \tag{4}$$

$$A_3^{i,0} \simeq 18\pi\alpha_s \left(r_\chi^{V_1} - r_\chi^{V_2} \right) \left[-(X_A^i)^2 + 2X_A^i - 4 + \frac{\pi^2}{3} \right], \tag{5}$$

$$A_3^{f,0} \simeq 18\pi\alpha_s \left(r_\chi^{V_1} + r_\chi^{V_2} \right) \left(2X_A^f - 1 \right) \left(2 - X_A^f \right), \tag{6}$$

for the non-vanishing longitudinal contributions, and

$$A_1^{i,+} \simeq A_2^{i,+} \simeq 18\pi\alpha_s \frac{m_1 m_2}{m_B^2} \left[2(X_A^i)^2 - 3X_A^i + 6 - \frac{2\pi^2}{3} \right], \tag{7}$$

$$A_1^{i,-} \simeq A_2^{i,-} \simeq 18\pi\alpha_s \frac{m_1 m_2}{m_B^2} \left(\frac{1}{2} X_L^i + \frac{5}{2} - \frac{\pi^2}{3} \right), \tag{8}$$

$$A_3^{i,-} \simeq 18\pi\alpha_s \left(\frac{m_1}{m_2} r_\chi^{V_2} - \frac{m_2}{m_1} r_\chi^{V_1} \right) \left[(X_A^i)^2 - 2X_A^i + 2 \right], \tag{9}$$

$$A_3^{f,-} \simeq 18\pi\alpha_s \left(\frac{m_1}{m_2} r_\chi^{V_2} + \frac{m_2}{m_1} r_\chi^{V_1}\right)\left[2(X_A^f)^2 - 5X_A^f + 3\right], \tag{10}$$

for the transverse ones, where the superscripts $0\,, \pm$ refer to the vector-meson helicities. Here $r_\chi^V = \frac{2m_V f_V^\perp}{m_b f_V}$, with f_V and $f_V^\perp$ denoting the longitudinal and transverse vector-meson decay constants; m_B and $m_{1,2}$ are the masses of the initial and final states, respectively.

The two complex quantities X_A and X_L are introduced in Eqs. (4)–(10) to parameterize the endpoint divergence [cf. Eqs. (1), (2)]. In addition, we have distinguished the WA contributions with the gluon emitted either from the initial (marked by the superscript "i") or from the final state (marked by the superscript "f"), corresponding to the nonfactorizable and the factorizable annihilation topologies, respectively. For the factorizable annihilation topologies, as argued in Refs. [23,24], since all decay constants have been factorized out from the hadronic matrix elements, the building blocks $A_3^{f,0}$ and $A_3^{f,-}$ are independent of the initial states. However, for the nonfactorizable annihilation topologies, $X_{A,L}^i$ are generally non-universal for $B_{u,d}$ and B_s decays [23,24]. Besides, an additional complex quantity, $X_H(\rho_H, \phi_H) = X_A(\rho_A, \phi_A)|_{A\to H}$, is introduced to parameterize the endpoint divergence in the hard spectator-scattering (HSS) amplitudes (cf. Refs. [9,53] for details).

With the above prescriptions for the WA amplitudes, we consider in this paper the following $B_s \to VV$ decay modes[2]:

(i) $\Delta D = 1$ transition: the color-allowed tree-dominated $\bar{B}_s \to \rho^- K^{*+}$, the color-suppressed tree-dominated $\bar{B}_s \to \rho^0 K^{*0}$ and ωK^{*0}, as well as the penguin-dominated $\bar{B}_s \to \phi K^{*0}$ decay, the amplitudes of which are given, respectively, as [9,53]

$$\mathcal{A}^h_{\bar{B}_s\to\rho^- K^{*+}} = A^h_{K^*\rho}\left[\delta_{pu}\alpha_1^{p,h} + \alpha_4^{p,h} + \alpha_{4,\rm EW}^{p,h} + \beta_3^{p,h} - \frac{1}{2}\beta_{3,\rm EW}^{p,h}\right], \tag{11}$$

$$\sqrt{2}\mathcal{A}^h_{\bar{B}_s\to\rho^0 K^{*0}} = A^h_{K^*\rho}\left[\delta_{pu}\alpha_2^{p,h} - \alpha_4^{p,h} + \frac{3}{2}\alpha_{3,\rm EW}^{p,h} + \frac{1}{2}\alpha_{4,\rm EW}^{p,h} - \beta_3^{p,h} + \frac{1}{2}\beta_{3,\rm EW}^{p,h}\right], \tag{12}$$

$$\sqrt{2}\mathcal{A}^h_{\bar{B}_s\to\omega K^{*0}} = A^h_{K^*\omega}\left[\delta_{pu}\alpha_2^{p,h} + 2\alpha_3^{p,h} + \alpha_4^{p,h} + \frac{1}{2}\alpha_{3,\rm EW}^{p,h} - \frac{1}{2}\alpha_{4,\rm EW}^{p,h} + \beta_3^{p,h} - \frac{1}{2}\beta_{3,\rm EW}^{p,h}\right], \tag{13}$$

$$\mathcal{A}^h_{\bar{B}_s\to\phi K^{*0}} = A^h_{K^*\phi}\left[\alpha_3^{p,h} - \frac{1}{2}\alpha_{3,\rm EW}^{p,h}\right] + A^h_{\phi K^*} \times \left[\alpha_4^{p,h} - \frac{1}{2}\alpha_{4,\rm EW}^{p,h} + \beta_3^{p,h} - \frac{1}{2}\beta_{3,\rm EW}^{p,h}\right]. \tag{14}$$

(ii) $\Delta S = 1$ transition: the penguin-dominated $\bar{B}_s \to K^{*+}K^{*-}$, $K^{*0}\bar{K}^{*0}$, and $\phi\phi$, $\rho^0\phi$, $\omega\phi$, as well as the pure annihilation $\bar{B}_s \to \rho^+\rho^-$, $\rho^0\rho^0$, $\rho\omega$, $\omega\omega$ decays, the amplitudes of which are given, respectively, as [9,53]

$$\mathcal{A}^h_{\bar{B}_s\to\bar{K}^{*-}K^{*+}} = A^h_{K^*\bar{K}^*}\left[\delta_{pu}\alpha_1^{p,h} + \alpha_4^{p,h} + \alpha_{4,\rm EW}^{p,h}\right] + B^h_{\bar{K}^*K^*}\left[\delta_{pu}b_1^{p,h} + b_3^{p,h} + 2b_4^{p,h} - \frac{1}{2}b_{3,\rm EW}^{p,h} + \frac{1}{2}b_{4,\rm EW}^{p,h}\right], \tag{15}$$

$$\mathcal{A}^h_{\bar{B}_s\to\bar{K}^{*0}K^{*0}} = A^h_{K^*\bar{K}^*}\left[\alpha_4^{p,h} - \frac{1}{2}\alpha_{4,\rm EW}^{p,h}\right] + B^h_{\bar{K}^*K^*}\left[b_3^{p,h} + 2b_4^{p,h} - \frac{1}{2}b_{3,\rm EW}^{p,h} - b_{4,\rm EW}^{p,h}\right], \tag{16}$$

$$\frac{1}{2}\mathcal{A}^h_{\bar{B}_s\to\phi\phi} = A^h_{\phi\phi}\left[\alpha_3^{p,h} + \alpha_4^{p,h} - \frac{1}{2}\alpha_{3,\rm EW}^{p,h} - \frac{1}{2}\alpha_{4,\rm EW}^{p,h} + \beta_3^{p,h} + \beta_4^{p,h} - \frac{1}{2}\beta_{3,\rm EW}^{p,h} - \frac{1}{2}\beta_{4,\rm EW}^{p,h}\right], \tag{17}$$

$$\sqrt{2}\mathcal{A}^h_{\bar{B}_s\to\rho^0\phi} = A^h_{\phi\rho}\left[\delta_{pu}\alpha_2^{p,h} + \frac{3}{2}\alpha_{3,\rm EW}^{p,h}\right], \tag{18}$$

$$\mathcal{A}^h_{\bar{B}_s\to\omega\phi} = \sqrt{2}A^h_{\phi\omega}\left[\delta_{pu}\alpha_2^{p,h} + 2\alpha_3^{p,h} + \frac{1}{2}\alpha_{3,\rm EW}^{p,h}\right], \tag{19}$$

$$\mathcal{A}^h_{\bar{B}_s\to\rho^0\rho^0} = B^h_{\rho\rho}\left[\delta_{pu}b_1^{p,h} + 2b_4^{p,h} + \frac{1}{2}b_{4,\rm EW}^{p,h}\right], \tag{20}$$

$$\mathcal{A}^h_{\bar{B}_s\to\rho^+\rho^-} = B^h_{\rho^-\rho^+}\left[\delta_{pu}b_1^{p,h} + b_4^{p,h} + b_{4,\rm EW}^{p,h}\right] + B^h_{\rho^+\rho^-}\left[b_4^{p,h} - \frac{1}{2}b_{4,\rm EW}^{p,h}\right], \tag{21}$$

$$\mathcal{A}^h_{\bar{B}_s\to\rho^0\omega} = B^h_{\rho\omega}\left[\delta_{pu}b_1^{p,h} + \frac{3}{2}b_{4,\rm EW}^{p,h}\right], \tag{22}$$

$$\mathcal{A}^h_{\bar{B}_s\to\omega\omega} = B^h_{\omega\omega}\left[\delta_{pu}b_1^{p,h} + 2b_4^{p,h} + \frac{1}{2}b_{4,\rm EW}^{p,h}\right]. \tag{23}$$

In the above decay amplitudes, the vertex, penguin and spectator-scattering corrections are encoded in the effective coefficients $\alpha_i^{p,h}$ (cf. Refs. [9,53] for details), and the WA contributions are denoted by $\beta_i^{p,h}$ (or $b_i^{p,h}$), which are defined, respectively, by [9,53]

[2] The expressions for the decay amplitudes given below should be multiplied with $V_{pb}V_{pd}^*$ (for $\Delta D = 1$ transition) and $V_{pb}V_{ps}^*$ (for $\Delta S = 1$ transition) and summed over $p = u, c$.

$$\beta_i^{p,h} = b_i^{p,h} B^h_{M_1M_2}/A^h_{M_1M_2}, \tag{24}$$

$$b_1^h = \frac{C_F}{N_c^2} C_1 A_1^{i,h}, \quad b_2^h = \frac{C_F}{N_c^2} C_2 A_1^{i,h}, \tag{25}$$

$$b_3^{p,h} = \frac{C_F}{N_c^2}\left[C_3 A_1^{i,h} + C_5(A_3^{i,h} + A_3^{f,h}) + N_c C_6 A_3^{f,h}\right], \tag{26}$$

$$b_4^{p,h} = \frac{C_F}{N_c^2}\left[C_4 A_1^{i,h} + C_6 A_2^{i,h}\right], \tag{27}$$

$$b_{3,\mathrm{EW}}^{p,h} = \frac{C_F}{N_c^2}\left[C_9 A_1^{i,h} + C_7(A_3^{i,h} + A_3^{f,h}) + N_c C_8 A_3^{f,h}\right], \tag{28}$$

$$b_{4,\mathrm{EW}}^{p,h} = \frac{C_F}{N_c^2}\left[C_{10} A_1^{i,h} + C_8 A_2^{i,h}\right]. \tag{29}$$

Based on the previous studies [22,53] and the amplitudes given above, $B_s \to VV$ decay modes can be classified as follows according to their sensitivities to the WA and/or HSS corrections:

- The pure annihilation decay modes: Because both WA and HSS corrections involve the undetermined endpoint contributions, the interference between them presents an obstacle for precisely probing the WA contributions from data. Fortunately, such problem can be avoided by using the pure annihilation decay modes, which can easily be seen from Eqs. (20), (21), (22) and (23). In this paper, the $\bar{B}_s \to \rho^0\rho^0$, $\rho^+\rho^-$, $\rho^0\omega$ and $\omega\omega$ decays belong to this category, but unfortunately, they have not been measured for now.
- The color-suppressed tree- and electroweak or QCD flavor-singlet penguin-dominated decays: Only two decay modes fall into this category, namely, $\bar{B}_s \to \rho^0\phi$ and $\omega\phi$. From Eqs. (18) and (19), one can find that these decays are characterized by an interplay of the color- and CKM-suppressed tree amplitude, α_2, electroweak penguin amplitude, $\alpha^c_{3,\mathrm{EW}}$, and flavor-singlet QCD penguin amplitude, α^c_3. For $\bar{B}_s \to \omega\phi$ decay, due to a partial cancellation between the QCD and electroweak penguin contributions, the largest partial amplitude is α_2 [53], which is very sensitive to the HSS corrections. For $\bar{B}_s \to \rho^0\phi$ decay, α_2 is also nontrivial even though it is numerically smaller than $\alpha^c_{3,\mathrm{EW}}$ when ρ_H is small. More importantly, a remarkable feature of such two decays is that their amplitudes are irrelevant to the WA contributions, and therefore very suitable for probing the HSS corrections. Recently, the branching ratio of $\bar{B}_s \to \rho^0\phi$ decay has been measured by the LHCb collaboration with a statistical significance of about 4σ [57].
- The color-suppressed tree-dominated $\Delta D = 1$ decays: This class includes $\bar{B}_s \to \rho^0 K^{*0}$ and ωK^{*0} decays, whose amplitudes are given by Eqs. (12) and (13), respectively. The CKM-factors relevant to the effective coefficients in their amplitudes are at the same order, $\sim \lambda^3$, and therefore one can roughly find that α_2 dominates their amplitudes. Further considering the fact that the HSS contribution in α_2 is proportional to the largest Wilson coefficient C_1, we can generally expect that these decays present strong constraints on the HSS endpoint parameters even though they are not as "clean" as $\bar{B}_s \to \rho^0\phi$ decay due to the interference induced by β^c_3. However, there is no available data for these decays for now.
- The QCD penguin-dominated decays: This class contains the residual decays, except for $\bar{B}_s \to \rho^- K^{*+}$, considered in this paper, among which $\bar{B}_s \to \phi K^{*0}$, $\phi\phi$ and $K^{*0}\bar{K}^{*0}$ decays have been measured. From their amplitudes, Eqs. (14), (16) and (17), one can find that the effective color-allowed QCD penguin amplitude, $\hat{\alpha}^c_4 \equiv \alpha^c_4 + \beta^c_3$, plays a dominant role [53]; and the penguin-annihilation amplitude, β^c_4, presents the first subdominant contribution besides $\hat{\alpha}^c_4$ for the longitudinal amplitude of the last two decay modes [53]. Further considering the fact that the HSS contribution in α^c_4 is trivial compared to the LO contribution $C_4 + C_3/N_C$, we can generally conclude that such three QCD penguin-dominated decays are suitable for probing the WA contribution from data even though they are not as "clean" as the pure annihilation decay modes.
  It should be noted that such an expectation or such a conclusion is valid only when ρ_H is not very large, especially for the decays involving α^c_3, for instance, $\bar{B}_s \to \phi K^{*0}$ and $\phi\phi$ decays. The HSS correction in α^c_3 with a large ρ_H can bring about a significant correction.
- The color-allowed tree-dominated $\Delta D = 1$ decay: In this paper, only $\bar{B}_s \to \rho^- K^{*+}$ decay belongs to this class. For this decay mode, the effects of HSS and WA contributions are generally not very significant, because of the dominant role played by the color-allowed tree amplitude, α_1. It also has not been measured.

2.2 Observables

Using the amplitudes given above, the observables for $B_s \to VV$ decays can be defined as follows. The most important observables are the CP-averaged branching ratio and direct CP-asymmetry, which are defined theoretically as [22]

$$\mathcal{B}[B_s \to f] = \frac{\tau_{B_s}}{2}\left(\Gamma[\bar{B}_s \to \bar{f}] + \Gamma[B_s \to f]\right), \tag{30}$$

$$\mathcal{A}_{\mathrm{CP}} = \frac{\Gamma[\bar{B}_s \to \bar{f}] - \Gamma[B_s \to f]}{\Gamma[\bar{B}_s \to \bar{f}] + \Gamma[B_s \to f]}, \tag{31}$$

respectively. The decay rates should be summed over the polarization state ($h' = L, \parallel, \perp$) for evaluating the "whole" observables. Following the convention of Ref. [53], the polarization amplitudes can easily be obtained from the helic-

ity amplitudes through the relations $\bar{A}_L = \bar{A}_0$ and $\bar{A}_{\parallel,\perp} = \frac{\bar{A}_- \pm \bar{A}_+}{\sqrt{2}}$.

Besides branching ratio and CP-asymmetry given by Eqs. (30) and (31), the two-body $B_s \to VV$ decays with cascading decays $V \to PP$ provide additional observables in the full angular analysis of the 4-body final state [58]. There are polarization fractions and relative phases defined by

$$f_{h'}^{\bar{B}_s} = \frac{|\bar{A}_{h'}|^2}{\sum_{h''} |\bar{A}_{h''}|^2}, \quad \phi_{\parallel,\perp}^{\bar{B}_s} = \arg \frac{\bar{A}_{\parallel,\perp}}{\bar{A}_L}, \tag{32}$$

for $\bar{B}_s$ decays. The same quantities for B_s decays are obtained by replacement $\bar{A}_{h'} \to A_{h'}$. The CP-averaged polarization fractions and CP-asymmetries are given, respectively, by

$$f_{h'} = \frac{f_{h'}^{\bar{B}_s} + f_{h'}^{B_s}}{2}, \quad A_{\rm CP}^{h'} = \frac{f_{h'}^{\bar{B}_s} - f_{h'}^{B_s}}{f_{h'}^{\bar{B}_s} + f_{h'}^{B_s}}, \tag{33}$$

in which only two of the polarization fractions are independent due to the normalization condition $f_L + f_\parallel + f_\perp = 1$; such a definition for $A_{\rm CP}^{h'}$ is in fact the same as Eq. (31) for a given h'. The CP-averaged and CP-violating observables for the relative phases can be constructed, respectively, as

$$\phi_{h'} = \frac{1}{2}\left(\phi_{h'}^{\bar{B}_s} + \phi_{h'}^{B_s}\right) - \pi\, \text{sign}(\phi_{h'}^{\bar{B}_s} + \phi_{h'}^{B_s}) \times \theta(|\phi_{h'}^{\bar{B}_s} - \phi_{h'}^{B_s}| - \pi), \tag{34}$$

$$\Delta\phi_{h'} = \frac{1}{2}\left(\phi_{h'}^{\bar{B}_s} - \phi_{h'}^{B_s}\right) + \pi\,\theta\left(|\phi_{h'}^{\bar{B}_s} - \phi_{h'}^{B_s}| - \pi\right), \tag{35}$$

for $h' = \parallel, \perp$. This phase convention for the amplitudes implies $\phi_{h'} = \Delta\phi_{h'} = 0$ at leading order, where all strong phases are zero [53], while it should be noted that the sign of A_L relative to the transverse amplitudes differs from the experimental convention, which leads to an offset of π for $\phi_{\parallel,\perp}$ [22,53].

It should be noted that the above "theoretical" definitions are in the flavor-eigenstate basis and at $t = 0$. The fact complicating the concept of B_s decay observables is caused by the significant effects of time-dependent oscillation between $\bar{B}_s$ and B_s states. Concerning the decays of $\bar{B}_s$ and B_s mesons into a common final state, $\bar{f} = f$, the untagged decay rate is the sum of the two time-dependent components, $\Gamma[\bar{B}_s(t) \to f] + \Gamma[B_s(t) \to f]$ [59,60], which yields the averaged and time-integrated branching ratio [59]

$$\widehat{\mathcal{B}}[B_s \to f_{h'}] = \frac{1}{2}\left(\frac{R_{f_{h'}}^H}{\Gamma_s^H} + \frac{R_{f_{h'}}^L}{\Gamma_s^L}\right) = \frac{\tau_{B_s}}{2}(R_{f_{h'}}^H + R_{f_{h'}}^L)\left[\frac{1 + y_s H_{f_{h'}}}{1 - y_s^2}\right], \tag{36}$$

where $R_{f_{h'}}^{H,L} \equiv \Gamma[B_s^{H,L} \to f_{h'}]$ with the heavy and light mass-eigenstates, $|B_s^{H,L}\rangle = p|B_s\rangle \mp q|\bar{B}_s\rangle$; $\tau_{B_s} \equiv \Gamma_s^{-1} = 2/(\Gamma_s^L + \Gamma_s^H)$ is the mean lifetime; $H_{f_{h'}} = (R_{f_{h'}}^H - R_{f_{h'}}^L)/(R_{f_{h'}}^H + R_{f_{h'}}^L)$ is the CP-asymmetry due to the width difference, and y_s is the parameter proportional to the width difference

$$y_s \equiv \frac{\Delta\Gamma_s}{2\Gamma_s} \equiv \frac{\Gamma_s^L - \Gamma_s^H}{2\Gamma_s}. \tag{37}$$

Then the relation between the experimentally measurable and theoretically calculated branching fractions, $\widehat{\mathcal{B}}[B_s \to f_{h'}]$ and $\mathcal{B}[B_s \to f_{h'}]$, can be written as [22,59]

$$\widehat{\mathcal{B}}[B_s \to f_{h'}] = \frac{1 + y_s H_{f_{h'}}}{1 - y_s^2}\mathcal{B}[B_s \to f_{h'}], \quad \widehat{\mathcal{B}}[B_s \to f] = \sum_{h'=L,\parallel,\perp} \widehat{\mathcal{B}}[B_s \to f_{h'}]. \tag{38}$$

Here the decay width parameter y_s is universal for B_s decays and has been well measured, $y_s = 0.063 \pm 0.005$ [34]. However, the CP-asymmetry $H_{f_{h'}}$ is generally non-universal, not only for various B_s decay modes, but also for various polarization states. Moreover, its values in most of B_s decays are not measured. Therefore, we take the SM prediction [22]

$$H_{f_{h'}} = \frac{2\text{Re}(\lambda_{f_{h'}})}{1 + |\lambda_{f_{h'}}|^2}, \quad \lambda_{f_{h'}} = \frac{q}{p}\frac{\bar{A}_{f_{h'}}}{A_{f_{h'}}}. \tag{39}$$

Accordingly, the experimentally measurable polarization fractions should also be modified as

$$\widehat{f}_{h'} = \frac{\widehat{\mathcal{B}}[B_s \to f_{h'}]}{\widehat{\mathcal{B}}[B_s \to f]} = \frac{(1 + y_s H_{f_{h'}})\mathcal{B}[B_s \to f_{h'}]}{\sum_{h'}(1 + y_s H_{f_{h'}})\mathcal{B}[B_s \to f_{h'}]}; \tag{40}$$

they still satisfy the normalization condition $\widehat{f}_L + \widehat{f}_\parallel + \widehat{f}_\perp = 1$. In addition, such a correction induced by the B_s oscillation does not affect the definition for the three polarization-dependent CP-asymmetries given by Eq. (33).

In general, $-1 \leqslant H_{f_{h'}} \leqslant 1$, and therefore the difference between $\widehat{\mathcal{B}}[B_s \to f]$ and $\mathcal{B}[B_s \to f]$ can reach up to $\mathcal{O}(10\%)$ for final states that are CP-eigenstates, as has been observed for some cases [59]. On the other hand, for the case of a flavor-specific decay ($\bar{f} \neq f$), where $H_{f_{h'}} = 0$, the correction factor in Eq. (38) is simplified as $1/(1 - y_s^2)$, which implies a good approximation $\widehat{\mathcal{B}}[B_s \to f] \simeq \mathcal{B}[B_s \to f]$ due to $y_s^2 \sim 4 \times 10^{-3} \ll 1$. In the following sections, the hat symbol, "$\widehat{\ }$", is omitted for convenience.

3 Numerical results and discussions

With the theoretical formulas given above, we now present our numerical results and discussions. The values of the input parameters used in our evaluation are summarized in Table 1. So far, only some observables of $\bar{B}_s \to \rho^0\phi$, ϕK^{*0}, $\phi\phi$ and $K^{*0}\bar{K}^{*0}$ decays, including the CP-averaged branching ratios, the polarization fractions and the relative phases between different helicity amplitudes, have been measured. The experi-

Table 1 Values of the input parameters: Wolfenstein parameters, pole and running quark masses, decay constants, form factors, Gegenbauer moments and decay width parameter y_s

$A = 0.8250^{+0.0071}_{-0.0111}$, $\lambda = 0.22509^{+0.00029}_{-0.00028}$, $\bar{\rho} = 0.1598^{+0.0076}_{-0.0072}$, $\bar{\eta} = 0.3499^{+0.0063}_{-0.0061}$; [61]
$m_c = 1.67 \pm 0.07$ GeV, $m_b = 4.78 \pm 0.06$ GeV, $m_t = 174.2 \pm 1.4$ GeV,
$\frac{\bar{m}_s(\mu)}{\bar{m}_{u,d}(\mu)} = 27.3 \pm 0.7$, $\bar{m}_s(2\text{GeV}) = 96^{+8}_{-4}$ MeV, $\bar{m}_b(\bar{m}_b) = 4.18^{+0.04}_{-0.03}$ GeV; [35]
$f_{B_s} = 227.2 \pm 3.4$ MeV, $f_{K^*} = 204 \pm 7$ MeV, $f^{\perp}_{K^*} = 159 \pm 6$ MeV,
$f_\rho = 213 \pm 5$ MeV, $f^{\perp}_\rho = 160 \pm 7$ MeV, $f_\phi = 233 \pm 4$ MeV,
$f^{\perp}_\phi = 191 \pm 4$ MeV, $f_\omega = 197 \pm 8$ MeV, $f^{\perp}_\omega = 148 \pm 13$ MeV; [35,62,63]
$A_0^{B_s\to\phi} = 0.389 \pm 0.045$, $A_1^{B_s\to\phi} = 0.296 \pm 0.027$, $V^{B_s\to\phi} = 0.387 \pm 0.033$,
$A_0^{B_s\to K^*} = 0.314 \pm 0.048$, $A_1^{B_s\to K^*} = 0.230 \pm 0.025$, $V^{B_s\to K^*} = 0.296 \pm 0.030$; [63]
$a_1^{\parallel,\perp}(\phi) = 0$, $a_1^{\parallel,\perp}(\rho) = 0$, $a_1^{\parallel,\perp}(\omega) = 0$, $a_1^{\parallel,(\perp)}(K^*) = 0.06 \pm 0.04\,(0.04 \pm 0.03)$,
$a_2^{\parallel,(\perp)}(\phi) = 0.23 \pm 0.08\,(0.14 \pm 0.07)$, $a_2^{\parallel,(\perp)}(\rho) = 0.17 \pm 0.07\,(0.14 \pm 0.06)$,
$a_2^{\parallel,(\perp)}(\omega) = 0.15 \pm 0.12\,(0.14 \pm 0.12)$, $a_2^{\parallel,(\perp)}(K^*) = 0.16 \pm 0.09\,(0.10 \pm 0.08)$; [63,64]
$y_s = \Delta\Gamma_s/(2\Gamma_s) = 0.063 \pm 0.005$. [34]

Table 2 Experimental data for the measured observables of $\bar{B}_s \to \rho^0\phi$, $K^{*0}\bar{K}^{*0}$, ϕK^{*0} and $\phi\phi$ decays; and the deviations of theoretical results from data in cases I and II, i.e., the $\chi_i\sigma_i$ (i denotes a given observable) evaluated at the best-fit points of $(\rho_A^{i,f}, \phi_A^{i,f})$ with the other inputs given by Eq. (42) and Table 1

Observable	Decay mode	Exp. [34]	Case I	Case II
$\mathcal{B}[10^{-6}]$	$\bar{B}_s \to \rho^0\phi$	0.27 ± 0.07	$+0.71\,\sigma$	$+0.71\,\sigma$
	$\bar{B}_s \to K^{*0}\bar{K}^{*0}$	10.8 ± 2.6	$+4.31\,\sigma$	$0.00\,\sigma$
	$\bar{B}_s \to \phi K^{*0}$	1.13 ± 0.30	$\mathbf{-2.57\,\sigma}$	$\mathbf{-3.17\,\sigma}$
	$\bar{B}_s \to \phi\phi$	18.6 ± 1.6	$0.00\,\sigma$	$0.00\,\sigma$
$f_L[\%]$	$\bar{B}_s \to K^{*0}\bar{K}^{*0}$	20.1 ± 7.0	$+5.99\,\sigma$	$+0.13\,\sigma$
	$\bar{B}_s \to \phi K^{*0}$	51 ± 17	$+0.41\,\sigma$	$0.00\,\sigma$
	$\bar{B}_s \to \phi\phi$	36.1 ± 2.2	$0.00\,\sigma$	$0.00\,\sigma$
$f_\perp[\%]$	$\bar{B}_s \to K^{*0}\bar{K}^{*0}$	58.4 ± 8.5	$-4.96\,\sigma$	$-1.21\,\sigma$
	$\bar{B}_s \to \phi K^{*0}$	28 ± 12	$-0.50\,\sigma$	$0.00\,\sigma$
	$\bar{B}_s \to \phi\phi$	30.6 ± 2.3	$0.00\,\sigma$	$0.00\,\sigma$
$\phi_\parallel + \pi$	$\bar{B}_s \to \phi K^{*0}$	$1.75^{+0.70}_{-0.61}$	$0.00\,\sigma$	$+0.31\,\sigma$
	$\bar{B}_s \to \phi\phi$	2.59 ± 0.15	$1.27\,\sigma$	$-0.27\,\sigma$

Bold values denote the largest deviation in the fit

mental data on these measured observables [34] are listed in the "Exp." column of Table 2 and will be used as constraints in the following χ^2-fits.

In order to probe the HSS and WA contributions in charmless $B_s \to VV$ decays, we perform χ^2-analyses for the endpoint parameters, adopting the statistical fitting approach illustrated in our previous work [25] (cf. Appendix C of Ref. [25] for detail). In the coming fits and posterior prediction, we have to evaluate the theoretical uncertainties induced by the inputs listed in Table 1. The total theoretical errors are obtained by evaluating separately the uncertainties induced by each input parameter and then adding them in quadrature.

Our χ^2-fits are based on the topology-dependent parametrization scheme for the endpoint divergence [23,24]. This implies that we need four free parameters $(\rho_A^{i,f}, \phi_A^{i,f})$ (where the superscripts i and f, as introduced in Sect. 2, correspond to the nonfactorizable and factorizable annihilation topologies, respectively) to describe the WA contributions. Besides, we also need two free parameters (ρ_H, ϕ_H) to describe the HSS contributions.

3.1 Constraints on (ρ_H, ϕ_H) from $\bar{B}_s \to \rho^0\phi$ decay

As has been illustrated in Refs. [1,2,22], the factor $\rho_H e^{i\phi_H}$ summarizes the remainder of the non-perturbative contribution including a possible strong phase; the numerical size of such a complex parameter is unknown. However, a too large value of ρ_H will give rise to numerically enhanced subleading $\Lambda_{\rm QCD}/m_b$ contributions compared with the formally leading terms. Thus, the size of ρ_H should be carefully coped with.

As analyzed in the last section, the $\bar{B}_s \to \rho^0\phi$ decay is independent of WA contributions and sensitive to HSS corrections. Therefore, it provides an ideal channel for probing the endpoint parameters in the HSS amplitudes. Recently, the branching ratio of $\bar{B}_s \to \rho^0\phi$ decay has been measured by

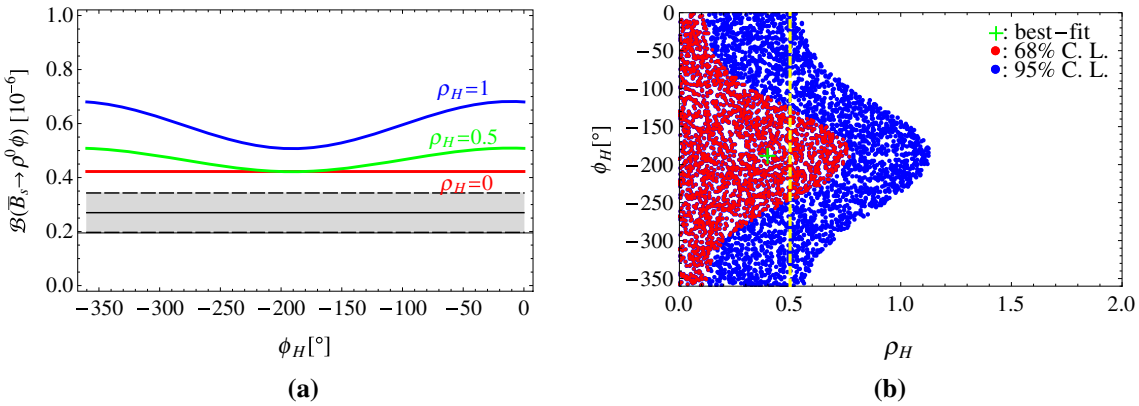

Fig. 1 **a** is the dependence of $\mathcal{B}(\bar{B}_s \to \rho^0\phi)$ on ϕ_H with different ρ_H labeled in the figure; the *gray band* is the experimental data within $1\,\sigma$ error bars **b** is the allowed spaces of (ρ_H, ϕ_H) at 68% C.L. and 95% C.L. under the constraint from the measured $\mathcal{B}(\bar{B}_s \to \rho^0\phi)$; the *dashed line* corresponds to $\rho_H = 0.5$, and the best-fit point corresponds to $\chi^2_{\rm min} = 0.19$

the LHCb collaboration [57],

$$\mathcal{B}(\bar{B}_s \to \rho^0\phi) = (2.7 \pm 0.7_{\rm stat.} \pm 0.2_{\rm syst.}) \times 10^{-7}, \qquad (41)$$

with a significance of about 4σ.

Taking $\rho_H = 0, 0.5, 1$ and using the central values of input parameters in Table 1, the dependence of the theoretical result for $\mathcal{B}(\bar{B}_s \to \rho^0\phi)$ on ϕ_H is shown in Fig. 1a. It can be clearly seen that the measured $\mathcal{B}(\bar{B}_s \to \rho^0\phi)$ presents a very stringent constraint on ρ_H; the large ρ_H should obviously be ruled out. The fitted space for (ρ_H, ϕ_H) is shown in Fig. 1b. We find that: (i) The large $\rho_H \gtrsim 0.75\,(1.15)$ is excluded at 68% (95%) C.L.. (ii) The bound of ϕ_H cannot be well determined due to the lack of data for the other observables; however, if $\rho_H \gtrsim 0.5$, values of ϕ_H around $-180°$ are favored.

It has been noted that, besides the $\bar{B}_s \to \rho^0\phi$ decay, the large ρ_H is also disfavored by the color-suppressed tree-dominated $B_d \to \rho^0\rho^0$ decay [29] even though a large HSS correction with large ρ_H is helpful for explaining the "πK and $\pi\pi$ puzzle" [25]. In the following analysis and evaluation, we take a conservative choice that

$$\rho_H = 0.5, \quad \phi_H[°] = -180 \pm 100, \qquad (42)$$

as inputs. Even though such a ϕ_H has a large uncertainty, its effect on the following analysis for $(\rho_A^{i,f}, \phi_A^{i,f})$ would be not significant because the HSS contribution with $\rho_H = 0.5$ is severely suppressed.

3.2 Case I: constraints on (ρ_A, ϕ_A) from $\bar{B}_s \to \phi K^{*0}$ and $\phi\phi$ decays

As can be seen from Eqs. (14) and (17), the $\bar{B}_s \to \phi K^{*0}$ and $\phi\phi$ decays have similar amplitude structures. However, being a $\Delta D = 1$ transition, the $\bar{B}_s \to \phi K^{*0}$ decay amplitude is suppressed by one power of the Wolfenstein parameter $\lambda \simeq 0.23$ compared with that of $\bar{B}_s \to \phi\phi$. This explains why the branching ratio $\mathcal{B}(\bar{B}_s \to \phi K^{*0})$ should be much smaller than $\mathcal{B}(\bar{B}_s \to \phi\phi)$. One can see from Tables 2 and 3 that the previous QCDF [19,53] and pQCD [65] predictions are in good agreement with each other for $\mathcal{B}(\bar{B}_s \to \phi\phi)$ and $\mathcal{B}(\bar{B}_s \to \phi K^{*0})$; in addition, their predictions are consistent with the data for the former, but they are much smaller than the data for the latter. Such a deviation could possibly be moderated by the different WA contributions involved in these two decays [cf. Eqs. (14) and (17)]. To this end, we firstly take the measured $\bar{B}_s \to \phi K^{*0}, \phi\phi$ decays as constraints to fit the WA contributions, which is named "case I" for convenience in the discussion.

Under the constraints from the measured $\bar{B}_s \to \phi K^{*0}$ and $\phi\phi$ decays (there are totally eight observables available, see Table 2), the allowed spaces of (ρ_A^i, ϕ_A^i) and (ρ_A^f, ϕ_A^f) are shown in Fig. 2. We find that:

- As shown in Fig. 2a, b, the spaces of (ρ_A^i, ϕ_A^i) and (ρ_A^f, ϕ_A^f) are bounded into three and two separate regions, respectively, at 68% C.L., which are labeled SI-1, 2, 3 and SF-1, 2 for convenience of discussion. We do not find any direct correspondence between SF-1, 2 for (ρ_A^f, ϕ_A^f) and SI-1, 2, 3 for (ρ_A^i, ϕ_A^i).[3]
- For (ρ_A^f, ϕ_A^f), as shown in Fig. 2b, the space of SF-1 is strictly bounded at 68% C.L., while the constraint on the one of SF-2 is very loose. The best-fit point with $\chi^2_{\rm min}/n_{\rm dof} = 8.6/4$ falls in SF-1; numerically,

$$(\rho_A^f, \phi_A^f)_{\text{best-fit}} = (1.31, -195°) \quad \text{SF-1}. \qquad (43)$$

[3] For instance, if we pick out the allowed space of SF-1 at 68% C.L. for (ρ_A^f, ϕ_A^f), all of the three solutions SI-1,2,3 for (ρ_A^i, ϕ_A^i) are still allowed.

Table 3 Theoretical results for the measured $\bar{B}_s \to K^{*0}\bar{K}^{*0}$, ϕK^{*0} and $\phi\phi$ decays

Observable	Decay mode	Case I	Case II	pQCD [65]	QCDF [53]	QCDF [19]
$\mathcal{B}[10^{-6}]$	$\bar{B}_s \to K^{*0}\bar{K}^{*0}$	$23.3^{+1.3}_{-1.3}$	$10.2^{+1.6+8.1}_{-0.9-6.3}$	$5.4^{+3.0}_{-2.4}$	$9.1^{+0.5+11.3}_{-0.4-6.8}$	$6.6^{+1.1+1.9}_{-1.4-1.7}$
	$\bar{B}_s \to \phi K^{*0}$	$0.22^{+0.14}_{-0.11}$	$0.11^{+0.07+0.06}_{-0.04-0.01}$	$0.39^{+0.20}_{-0.17}$	$0.4^{+0.1+0.5}_{-0.1-0.3}$	$0.37^{+0.06+0.24}_{-0.05-0.20}$
	$\bar{B}_s \to \phi\phi$	$19.2^{+3.3}_{-1.5}$	$18.4^{+7.8+11.9}_{-1.4-10.6}$	$16.7^{+8.9}_{-7.1}$	$21.8^{+1.1+30.4}_{-1.1-17.0}$	$16.7^{+2.6+11.3}_{-2.1-8.8}$
$A_{CP}[\%]$	$\bar{B}_s \to K^{*0}\bar{K}^{*0}$	$-0.1^{+0.0}_{-0.0}$	$0.1^{+0.1+0.2}_{-0.1-0.3}$	0.0	1^{+0+1}_{-0-0}	$0.4^{+0.8+0.6}_{-0.5-0.4}$
	$\bar{B}_s \to \phi K^{*0}$	$-29.0^{+9.0}_{-3.0}$	$-36.1^{+7.1+21.3}_{-5.2-4.2}$	0.0	-17^{+4+9}_{-5-9}	-9^{+3+4}_{-1-6}
	$\bar{B}_s \to \phi\phi$	0^{+0}_{-0}	$0.6^{+0.2+0.4}_{-0.2-0.4}$	0.0	1^{+0+1}_{-0-0}	$0.2^{+0.4+0.5}_{-0.3-0.2}$
$A^0_{CP}[\%]$	$\bar{B}_s \to K^{*0}\bar{K}^{*0}$	0^{+0}_{-0}	$-0.2^{+0.2+0.7}_{-0.2-0.8}$	0.0	0^{+0+0}_{-0-0}	–
	$\bar{B}_s \to \phi K^{*0}$	$-2.6^{+1.5}_{-2.2}$	$-21.1^{+12.2+26.2}_{-26.9-35.5}$	0.0	-9^{+2+16}_{-3-20}	–
	$\bar{B}_s \to \phi\phi$	$-0.9^{+0.2}_{-0.7}$	$0.3^{+0.2+2.0}_{-0.3-0.6}$	0.0	0^{+0+1}_{-0-0}	–
$A^{\perp}_{CP}[\%]$	$\bar{B}_s \to K^{*0}\bar{K}^{*0}$	$0.4^{+0.1}_{-0.1}$	$0.2^{+0.1+0.3}_{-0.1-0.3}$	0.0	–	–
	$\bar{B}_s \to \phi K^{*0}$	$8.7^{+3.3}_{-3.7}$	$19.5^{+5.1+1.4}_{-10.2-8.1}$	0.0	–	–
	$\bar{B}_s \to \phi\phi$	$0.6^{+0.1}_{-0.2}$	$0^{+0.2+0.7}_{-0.2-0.4}$	0.0	–	–
$f_L[\%]$	$\bar{B}_s \to K^{*0}\bar{K}^{*0}$	$67.1^{+1.2}_{-5.1}$	$27.7^{+8.2+9.5}_{-6.7-18.9}$	$38.3^{+12.1}_{-10.5}$	63^{+0+42}_{-0-29}	56^{+4+22}_{-7-26}
	$\bar{B}_s \to \phi K^{*0}$	$72.0^{+5.1}_{-14.0}$	$43.6^{+14.6+51.5}_{-24.0-25.3}$	$50.0^{+8.1}_{-7.2}$	40^{+1+67}_{-1-35}	43^{+2+21}_{-2-18}
	$\bar{B}_s \to \phi\phi$	$35.0^{+4.3}_{-19.0}$	$39.4^{+7.3+14.4}_{-6.6-29.1}$	$34.7^{+8.9}_{-7.1}$	43^{+0+61}_{-0-34}	36^{+3+23}_{-4-18}
$f_{\perp}[\%]$	$\bar{B}_s \to K^{*0}\bar{K}^{*0}$	$15.2^{+1.1}_{-1.0}$	$41.8^{+6.3+10.2}_{-5.7-14.0}$	$30.0^{+5.3}_{-6.1}$	–	–
	$\bar{B}_s \to \phi K^{*0}$	$13.4^{+8.6}_{-2.1}$	$25.9^{+8.4+14.4}_{-9.1-23.5}$	$24.2^{+3.6}_{-3.9}$	–	–
	$\bar{B}_s \to \phi\phi$	$30.0^{+4.2}_{-2.6}$	$33.0^{+7.0+17.2}_{-4.1-21.3}$	$31.6^{+3.5}_{-4.4}$	–	–
$\phi_{\parallel} + \pi$	$\bar{B}_s \to K^{*0}\bar{K}^{*0}$	$2.81^{+0.10}_{-0.11}$	$2.20^{+0.19+0.64}_{-0.19-0.40}$	$2.12^{+0.21}_{-0.25}$	$2.84^{+0+1.00}_{-0-0.54}$	–
	$\bar{B}_s \to \phi K^{*0}$	$1.82^{+0.46}_{-0.52}$	$2.77^{+0.66+1.33}_{-0.80-0.56}$	$1.95^{+0.21}_{-0.22}$	$2.71^{+0+1.00}_{-0-0.54}$	–
	$\bar{B}_s \to \phi\phi$	$3.09^{+0.26}_{-0.31}$	$2.38^{+0.17+1.13}_{-0.44-0.44}$	2.01 ± 0.23	$2.80^{+0+0.75}_{-0-0.50}$	–
$\phi_{\perp} + \pi$	$\bar{B}_s \to K^{*0}\bar{K}^{*0}$	$2.61^{+0.14}_{-0.15}$	$2.17^{+0.22+0.22}_{-0.20-0.32}$	–	–	
	$\bar{B}_s \to \phi K^{*0}$	$1.10^{+0.32}_{-0.32}$	$3.51^{+0.92+1.40}_{-1.10-0.48}$	–	–	
	$\bar{B}_s \to \phi\phi$	$4.70^{+0.27}_{-0.31}$	$0.53^{+0.24+0.61}_{-0.24-0.35}$	–	–	
$\Delta\phi_{\parallel}$	$\bar{B}_s \to K^{*0}\bar{K}^{*0}$	0^{+0}_{-0}	$0.01^{+0+0.01}_{-0-0}$	$0^{+0+0.09}_{-0-0.03}$	–	
	$\bar{B}_s \to \phi K^{*0}$	$-0.07^{+0.05}_{-0.05}$	$0.17^{+0.34+0.16}_{-0.19-0.20}$	$0.03^{+0+0.15}_{-0-0.06}$	–	
	$\bar{B}_s \to \phi\phi$	-0.01^{+0}_{-0}	$0^{+0+0.01}_{-0-0.01}$	0^{+0+0}_{-0-0}	–	
$\Delta\phi_{\perp}$	$\bar{B}_s \to K^{*0}\bar{K}^{*0}$	0^{+0}_{-0}	$0.01^{+0+0.01}_{-0-0}$	–	–	
	$\bar{B}_s \to \phi K^{*0}$	$-0.16^{+0.05}_{-0.05}$	$0.26^{+0.19+0.09}_{-0.24-0.06}$	–	–	
	$\bar{B}_s \to \phi\phi$	-0.01^{+0}_{-0}	$0.01^{+0+0.01}_{-0-0.01}$	–	–	

It should be noted that we also can find a point in SF-2, (0.45, −40°) [SF-2], having a χ^2 value similar to the $\chi^2_{\rm min}$ in SF-1. The situation for (ρ^i_A, ϕ^i_A) is similar to the one for (ρ^f_A, ϕ^f_A), but is much more complicated as Fig. 2a shows. The best-fit point in SI-1 is

$$(\rho^i_A, \phi^i_A)_{\text{best-fit}} = (5.75, -65^\circ) \qquad \text{SI-1}\,. \tag{44}$$

These allowed spaces in Fig. 2a, b will be further confronted with the measured observables of $\bar{B}_s \to K^{*0}\bar{K}^{*0}$ decay in the next subsection.

- The correlation, ρ^i_A vs. ρ^f_A, is shown by Fig. 2c. One can see again that ρ^f_A is significantly divided into two parts. The relation between ρ^f_A and ρ^i_A is not clear due to the large uncertainties except that they cannot be equal to zero simultaneously. The correlation, ϕ^i_A vs. ϕ^f_A, shown in Fig. 2d is very interesting. One can clearly see that the ϕ^i_A can be well determined except when $\phi^f_A \sim -30^\circ$ or -190° and vice versa; the case for ϕ^f_A is similar. Hence, the phases $\phi^{i,f}_A$ are expected to be well determined when more constraints are considered.

As argued in Refs. [23,24], the parameters (ρ^f_A, ϕ^f_A) are expected to be universal for the $B_{u,d}$ and B_s systems, while (ρ^i_A, ϕ^i_A) are flavor dependent on the initial states. Comparing with the fitted results in $B_{u,d}$ system [29], we find that

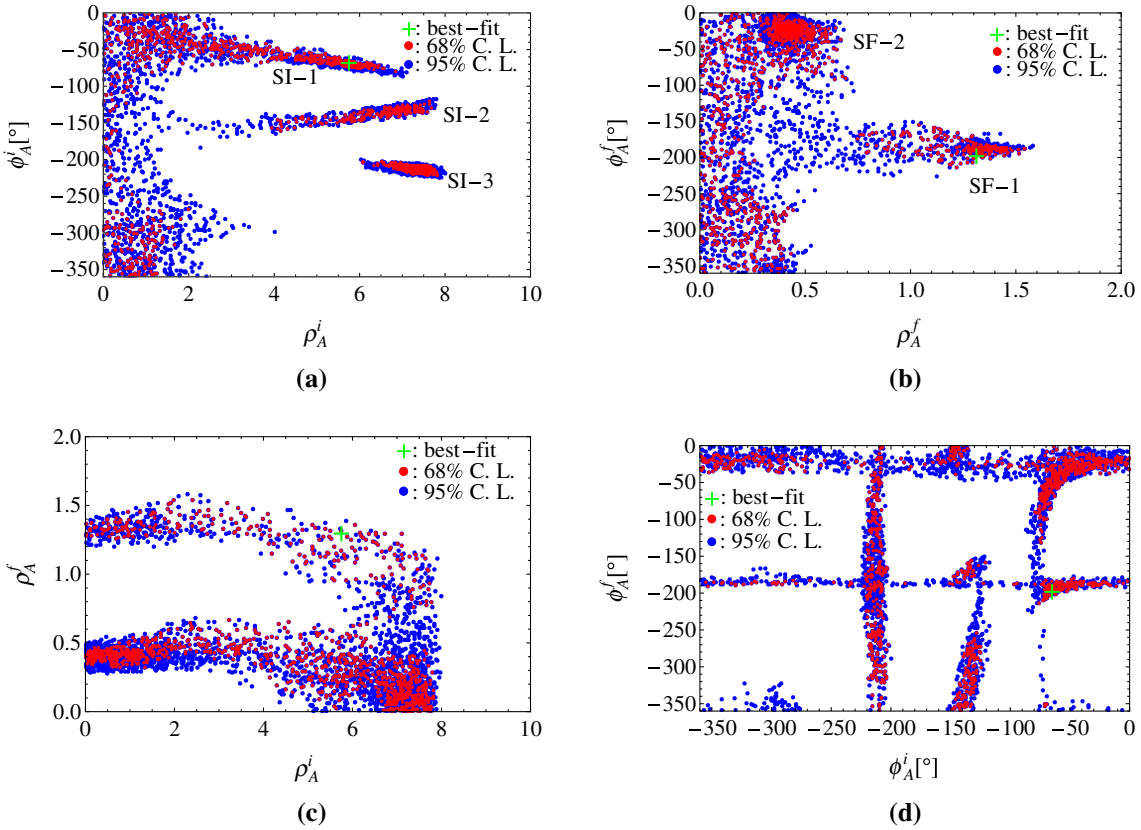

Fig. 2 The allowed spaces of $(\rho_A^{i,f}, \phi_A^{i,f})$ (**a**, **b**) at 68% C.L. and 95% C.L. under the constraints from the measured $\bar{B}_s \to \phi K^{*0}$ and $\phi\phi$ decays, namely, case I. The fitted spaces are also shown in (ρ_A^i, ρ_A^f) and (ϕ_A^i, ϕ_A^f) planes (**c**, **d**) in order to show the possible correlation. The best-fit point corresponds to $\chi^2_{\rm min}/n_{\rm dof} = 8.6/4$

the best-fit values, Eqs. (43) and (44), are very similar to the results, $(\rho_A^i, \phi_A^i)_{B_d} \simeq (5.80, -70°)$ and $(\rho_A^f, \phi_A^f)_{B_d} \simeq (1.19, -158°)$ (i.e., solution C given by Eq. (14) in Ref. [29]) obtained by fitting to $B_{u,d} \to \rho K^*$ and $\bar{K}^* K^*$ decays. However, it should be noted that the results in Ref. [29] are based on the assumption $(\rho_H, \phi_H) = (\rho_A^i, \phi_A^i)$, which is not employed in this paper because ρ_H is strictly constrained by $B_s \to \rho\phi$ decay as analyzed in the last subsection; thus, the flavor dependence of (ρ_A^i, ϕ_A^i) is indeterminable here.

The goodness of the fit can be characterized by $\chi^2_{\rm min}/n_{\rm dof}$ and p value.[4] Numerically, we obtain

$$\chi^2_{\rm min}/n_{\rm dof} = 8.6/4, \quad p\ \text{value} = 0.07 \tag{45}$$

at the best-fit point given by Eqs. (43) and (44). In order to find the observables which lead to the large $\chi^2_{\rm min}$ and small p value, we summarize the deviations of theoretical results from data for the considered observables in the fourth column of Table 2. It can be clearly seen that the tension between the theoretical result and data for $\mathcal{B}(\bar{B}_s \to \phi K^{*0})$, $\sim -2.57\,\sigma$, dominates the contributions to $\chi^2_{\rm min}$. Numerically, one can find $\chi^2_{\mathcal{B}(\bar{B}_s \to \phi K^{*0})}/\chi^2_{\rm min} = 77\%$. Such a tension implies that the problem of large $\mathcal{B}(\bar{B}_s \to \phi K^{*0})$ mentioned in the beginning of this subsection is hardly to be moderated by the WA contribution due to the constraints from the other measured observables. In addition, from Table 2, we also find some significant tensions in the $\bar{B}_s \to K^{*0}\bar{K}^{*0}$ decay, which is not considered in the fit in this case (case I). This implies that the best-fit points given by Eqs. (43) and (44) might be excluded when the constraints from $\bar{B}_s \to K^{*0}\bar{K}^{*0}$ decay are considered; and the other fitted spaces in this case may also suffer from challenges from $\bar{B}_s \to K^{*0}\bar{K}^{*0}$ decay, which will be studied in detail in the next two subsections.

3.3 Polarizations in $\bar{B}_s \to K^{*0}\bar{K}^{*0}$ decay

In the fit of case I, we do not include the measured $\bar{B}_s \to K^{*0}\bar{K}^{*0}$ decay, because it is difficult to understand its polarizations measured by the LHCb collaboration [66]. It is well known that, due to the $(V-A)$ nature of the SM weak interactions, the hierarchical pattern among the three helicity ampli-

[4] $n_{\rm dof}$ is the number of degrees of freedom given by the number of measurements minus the number of fitted parameters. In the evaluation of the p value, we assume that the goodness-of-fit statistic follows the χ^2 p.d.f. [35].

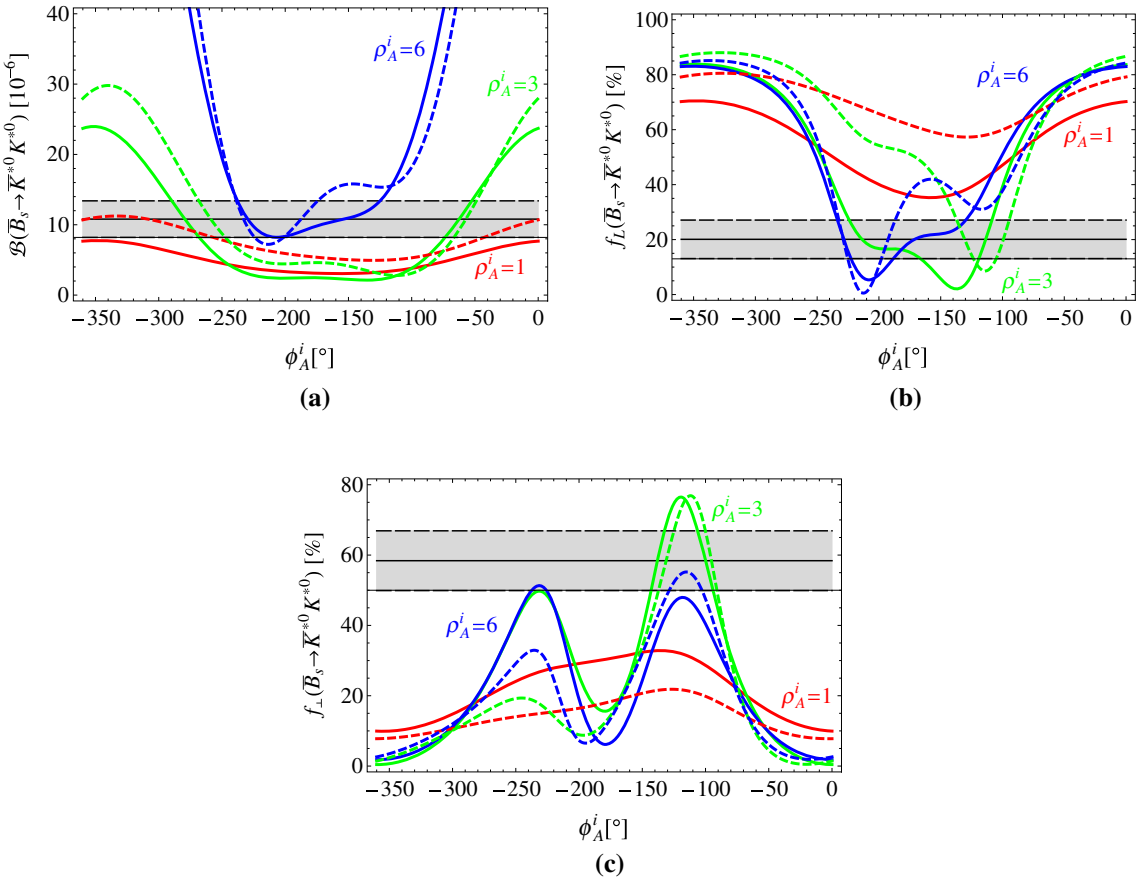

Fig. 3 The dependences of $\mathcal{B}(\bar{B}_s \to K^{*0}\bar{K}^{*0})$ and $f_{L,\perp}(\bar{B}_s \to K^{*0}\bar{K}^{*0})$ on the parameters (ρ_A^i, ϕ_A^i), with fixed $(\rho_A^f, \phi_A^f) = (1.31, -195°)$ (*solid lines*) and $(0.45, -40°)$ (*dashed lines*). The *shaded bands* are the experimental data within 1 σ error bars

tudes, $A_0 : A_- : A_+ = 1 : \frac{\Lambda_{\rm QCD}}{m_b} : (\frac{\Lambda_{\rm QCD}}{m_b})^2$, is expected in charmless $B \to VV$ decays [67]. Even after the QCD corrections are taken into account, the charmless $B \to VV$ decay amplitudes are generally still dominated by the longitudinal polarization component. For the penguin-dominated $B \to VV$ decays, the longitudinal polarization fraction is generally predicted at the level of about 50%, for instance in the $B \to \phi K^*$ decays [68–75]. Consistent with the above expectation, the longitudinal (transverse) polarization fraction, $f_{L(\perp)}(\bar{B}_s \to K^{*0}\bar{K}^{*0}) \sim 50\%\,(25\%)$, is predicted both in the QCDF [53] and in the pQCD approach [65]. However, the obviously different experimental results have been measured by the LHCb collaboration [66],

$$f_L(\bar{B}_s \to K^{*0}\bar{K}^{*0}) = (20.1 \pm 5.7 \pm 4.0)\%, \quad (46)$$

$$f_\parallel(\bar{B}_s \to K^{*0}\bar{K}^{*0}) = (21.5 \pm 4.6 \pm 1.5)\%, \quad (47)$$

which imply $f_\perp(\bar{B}_s \to K^{*0}\bar{K}^{*0}) = (58.4 \pm 8.5)\%$. Furthermore, these measurements are also inconsistent with the previous theoretical expectation, $f_\parallel \approx f_\perp$ (the relation $|f_\parallel - f_\perp| \lesssim 4\%$ is satisfied by most of the charmless $B \to VV$ decays [53]). As a consequence, these possible anomalies present a challenge to the current theoretical predictions. Therefore, we would like to check if the modifications of endpoint parameters could reconcile these anomalies.

In Fig. 3, we plot the dependences of $\mathcal{B}(\bar{B}_s \to K^{*0}\bar{K}^{*0})$ and $f_{L,\perp}(\bar{B}_s \to K^{*0}\bar{K}^{*0})$ on the parameters (ρ_A^i, ϕ_A^i) with $(\rho_A^f, \phi_A^f) = (1.31, -195°)$ and $(0.45, -40°)$, which are the best-fit values in SF-1 and -2, respectively, in case I. From Fig. 3, one can see that: (i) The small $\rho_A^i \lesssim 1$ is perhaps allowed by the measured $\mathcal{B}(\bar{B}_s \to K^{*0}\bar{K}^{*0})$ with ϕ_A^i around 0° (or −360°) as Fig. 3a shows, but is excluded by both $f_L(\bar{B}_s \to K^{*0}\bar{K}^{*0})$ and $f_\perp(\bar{B}_s \to K^{*0}\bar{K}^{*0})$ as Figs. 3b, c show. (ii) With $\rho_A^i \sim 3$, $\mathcal{B}(\bar{B}_s \to K^{*0}\bar{K}^{*0})$ and $f_{L,\perp}(\bar{B}_s \to K^{*0}\bar{K}^{*0})$ present different requirements for ϕ_A^i, which can be seen by comparing Fig. 3a with Fig. 3b, c. This implies that the choice $\rho_A^i \sim 3$ is also excluded by the anomalies of $f_{L,\perp}(\bar{B}_s \to K^{*0}\bar{K}^{*0})$. (iii) One can also find that only a large $\rho_A^i \sim 6$ with the phase $\phi_A^i \sim -240°$ or $-130°$ could possibly account for the current LHCb measurements for $f_{L,\perp}(\bar{B}_s \to K^{*0}\bar{K}^{*0})$. It is very interesting that such possible solutions are similar to SI-2 and -3 shown in Fig. 2a. However, SI-1 is possibly excluded by $f_{L,\perp}(\bar{B}_s \to K^{*0}\bar{K}^{*0})$. In order to further check such possible solutions, a combined fit for the endpoint parameters is performed with the mea-

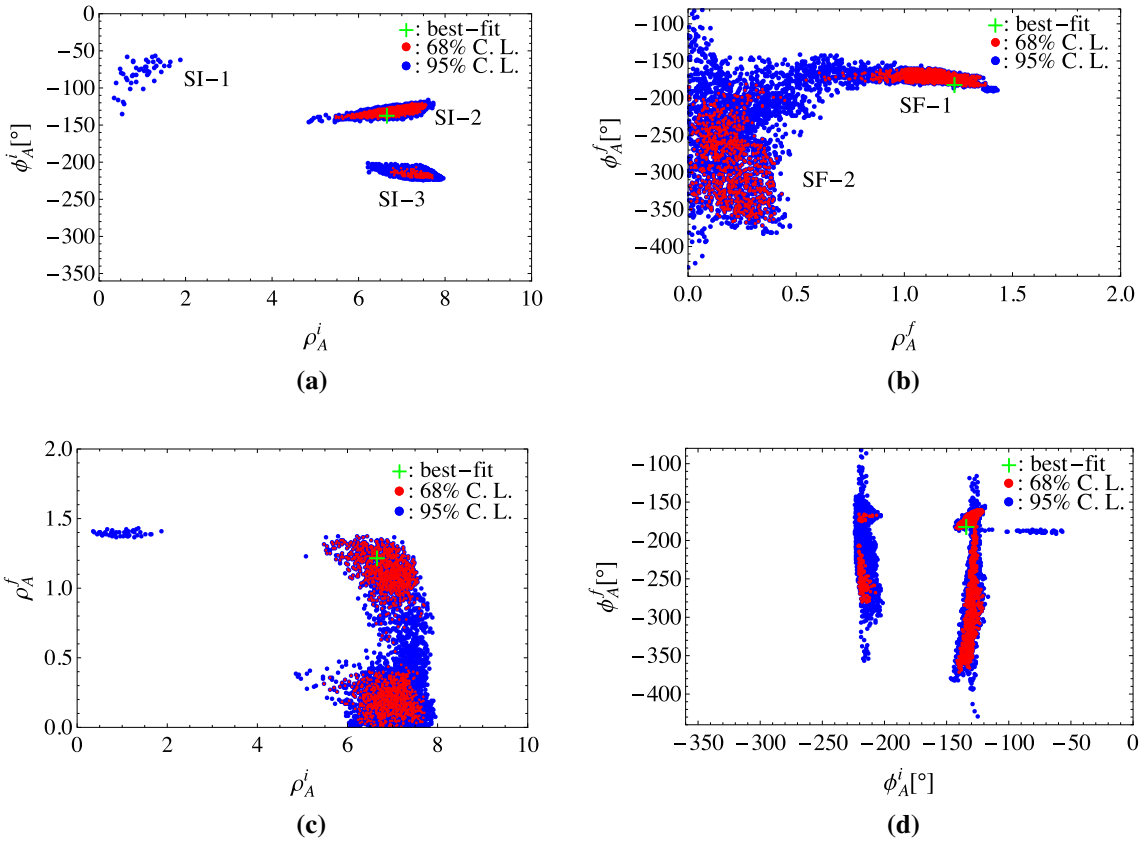

Fig. 4 The allowed spaces of $(\rho_A^{i,f}, \phi_A^{i,f})$ at 68% C.L. and 95% C.L. under the combined constraints from $\bar{B}_s \to \phi K^{*0}$, $\phi\phi$ and $K^{*0}\bar{K}^{*0}$ decays, namely, case II. The best-fit points correspond to $\chi^2_{min}/n_{\rm dof} = 11.2/7$

sured observables of $\bar{B}_s \to \phi K^{*0}$, $\phi\phi$ and $K^{*0}\bar{K}^{*0}$ decays as constraints.

3.4 Case II: combined fit to the measured $B_s \to VV$ decays

Under the combined constraints from $\bar{B}_s \to \phi K^{*0}$, $\phi\phi$ and $K^{*0}\bar{K}^{*0}$ decays (i.e., the measured 11 observables of $B_s \to VV$ decays are now included), our fitted results for the endpoint parameters are shown in Fig. 4, which is named "case II" for convenience in the discussion. It can be seen that:

- For (ρ_A^i, ϕ_A^i), because of the constraints from $f_{L,\perp}(\bar{B}_s \to K^{*0}\bar{K}^{*0})$, the space SI-1 favored in case I is excluded at 68% C.L. in case II, which can be clearly seen from Fig. 4a and easily understood from the analysis in Sect. 3.3, while both SI-2 and -3 survive, but they are further restricted; the large ρ_A^i is required to fit $f_{L,\perp}(\bar{B}_s \to K^{*0}\bar{K}^{*0})$. The spaces SI-2 and -3 are located symmetrically at two sides of $\phi_A^i \sim -180°$, and thus lead to a similar $|X_A^i|$ but to different signs of $\mathrm{Im}[X_A^i]$. In view of $\chi^2_{\rm min}$, SI-2 involving the best-fit point is much more favored. Numerically, we obtain

$$(\rho_A^i, \phi_A^i[°]) = (6.65^{+0.91}_{-1.17}, -134^{+13}_{-8})\,. \quad \text{SI-2} \qquad (48)$$

- For (ρ_A^f, ϕ_A^f), the two spaces, SF-1 and -2, are still allowed and further restricted in case II as Fig. 4b shows. Such two spaces at 68% C.L. can be clearly distinguished according to if $\rho_A^f \gtrsim 0.5$. The best-fit point falls in the space SF-1. For SF-1, the ranges of both ρ_A^f and ϕ_A^f are strictly bounded; numerically, we obtain

$$(\rho_A^f, \phi_A^f[°]) = (1.23^{+0.15}_{-0.62}, -179^{+19}_{-5})\,. \quad \text{SF-1} \qquad (49)$$

  For SF-2, even though the space of (ρ_A^f, ϕ_A^f) is further restricted compared with case I, the constraints are still very loose.
- The correlations, ρ_A^i vs. ρ_A^f and ϕ_A^i vs. ϕ_A^f, are shown by Fig. 4c, d, respectively. The main difference between case I and case II is that the ranges $\rho_A^i \lesssim 5.5$ and $\phi_A^i \gtrsim -140°$ or $-220°$ are excluded by the $\bar{B}_s \to K^{*0}\bar{K}^{*0}$ decay at 68% C.L. in case II.
  In addition, it also can be found that the relation $(\rho_A^i, \phi_A^i) \neq (\rho_A^f, \phi_A^f)$ is required at 68% C.L., which

Table 4 Theoretical results for the $b \to d$ induced $\bar{B}_s \to \rho^- K^{*+}$, $\rho^0 K^{*0}$ and ωK^{*0} decays

Observable	Decay mode	Case I	Case II	pQCD [65]	QCDF [53]	QCDF [19]
$\mathcal{B}[10^{-6}]$	$\bar{B}_s \to \rho^- K^{*+}$	$28.5^{+9.8}_{-8.3}$	$28.5^{+9.8\ +0.1}_{-8.4\ -0.1}$	$24.0^{+10.9+1.2+0.0}_{-8.7-1.4-2.4}$	$25.2^{+1.5+4.7}_{-1.7-3.1}$	$21.6^{+1.3+0.9}_{-2.8-1.5}$
	$\bar{B}_s \to \rho^0 K^{*0}$	$1.23^{+1.20}_{-0.63}$	$1.20^{+1.20\ +0.01}_{-0.57\ -0.01}$	$0.40^{+0.19+0.11+0.00}_{-0.15-0.07-0.03}$	$1.5^{+1.0+3.1}_{-0.5-1.5}$	$1.3^{+2.0+1.7}_{-0.6-0.3}$
	$\bar{B}_s \to \omega K^{*0}$	$1.16^{+1.07}_{-0.51}$	$1.14^{+1.05\ +0.03}_{-0.51\ -0.04}$	$0.35^{+0.16+0.09+0.04}_{-0.14-0.08-0.08}$	$1.2^{+0.7+2.3}_{-0.3-1.1}$	$1.1^{+1.5+1.3}_{-0.5-0.3}$
$A_{CP}[\%]$	$\bar{B}_s \to \rho^- K^{*+}$	$-9.1^{+1.0}_{-1.1}$	$-20.1^{+0.5\ +3.3}_{-0.6\ -1.3}$	$-9.1^{+1.4+1.0+0.2}_{-1.5-1.2-0.3}$	-3^{+1+2}_{-1-3}	-11^{+1+4}_{-1-1}
	$\bar{B}_s \to \rho^0 K^{*0}$	$-36.6^{+14.5}_{-17.0}$	$-18.0^{+11.3\ +3.7}_{-12.8\ -9.6}$	$62.7^{+6.4+10.5+7.5}_{-5.9-16.0-7.9}$	27^{+5+34}_{-7-27}	46^{+15+10}_{-17-25}
	$\bar{B}_s \to \omega K^{*0}$	$-36.5^{+12.3}_{-16.6}$	$-18.6^{+8.6\ +9.1}_{-14.4\ -3.6}$	$-78.1^{+2.9+13.1+8.1}_{-2.2-7.4-8.3}$	-34^{+10+31}_{-7-43}	-50^{+20+21}_{-15-6}
$A^0_{CP}[\%]$	$\bar{B}_s \to \rho^- K^{*+}$	$-1.5^{+0.5}_{-0.8}$	$-0.2^{+0.1\ +1.2}_{-0.1\ -0.4}$	$-2.71^{+0.68}_{-0.72}$	-2^{+1+6}_{-0-3}	–
	$\bar{B}_s \to \rho^0 K^{*0}$	$3.8^{+8.6}_{-6.6}$	$-5.4^{+13.3\ +4.5}_{-13.1\ -5.2}$	$-17.5^{+21.2}_{-13.0}$	-5^{+1+49}_{-0-18}	–
	$\bar{B}_s \to \omega K^{*0}$	$-5.3^{+5.0}_{-6.9}$	$3.1^{+8.8\ +4.3}_{-9.0\ -4.5}$	$-5.99^{+23.52}_{-50.21}$	6^{+1+19}_{-1-60}	–
$A^\perp_{CP}[\%]$	$\bar{B}_s \to \rho^- K^{*+}$	$35.4^{+3.8}_{-5.5}$	$-6.1^{+1.1\ +7.8}_{-1.5\ -6.3}$	$55.0^{+10.3}_{-10.5}$	–	–
	$\bar{B}_s \to \rho^0 K^{*0}$	$-34.5^{+41.8}_{-62.4}$	$46.3^{+52.0\ +26.4}_{-53.1\ -26.6}$	$22.0^{+29.9}_{-31.4}$	–	–
	$\bar{B}_s \to \omega K^{*0}$	$44.4^{+52.6}_{-17.6}$	$-33.1^{+58.1\ +32.3}_{-57.0\ -25.3}$	$6.95^{+27.91}_{-32.14}$	–	–
$f_L[\%]$	$\bar{B}_s \to \rho^- K^{*+}$	$94.7^{+1.6}_{-3.1}$	$94.8^{+1.6\ +0.2}_{-2.9\ -0.1}$	95^{+1+1+0}_{-1-1-0}	92^{+1+5}_{-1-8}	92^{+1+1}_{-2-3}
	$\bar{B}_s \to \rho^0 K^{*0}$	$83.5^{+10.2}_{-11.7}$	$85.0^{+9.5\ +1.2}_{-10.6\ -0.8}$	$57^{+6+6+1}_{-10-8-0}$	93^{+2+5}_{-3-54}	90^{+4+3}_{-5-23}
	$\bar{B}_s \to \omega K^{*0}$	$84.5^{+10.4}_{-11.5}$	$86.4^{+9.6\ +0.6}_{-10.1\ -0.6}$	$50^{+7+11+1}_{-8-15-1}$	93^{+2+5}_{-4-49}	90^{+3+3}_{-4-23}
$f_\perp[\%]$	$\bar{B}_s \to \rho^- K^{*+}$	$2.4^{+1.4}_{-0.8}$	$2.3^{+1.4\ +0.1}_{-0.8\ -0.1}$	$2.31^{+0.22}_{-0.21}$	–	–
	$\bar{B}_s \to \rho^0 K^{*0}$	$8.5^{+6.2}_{-5.4}$	$7.1^{+5.0\ +0.5}_{-4.5\ -0.6}$	$22.5^{+7.3}_{-4.7}$	–	–
	$\bar{B}_s \to \omega K^{*0}$	$8.1^{+6.2}_{-5.6}$	$6.4^{+4.9\ +0.4}_{-4.7\ -0.2}$	$26.1^{+9.8}_{-7.0}$	–	–
$\phi_\parallel + \pi$	$\bar{B}_s \to \rho^- K^{*+}$	$3.17^{+0.20}_{-0.22}$	$3.18^{+0.20\ +0.21}_{-0.22\ -0.23}$	$3.07^{+0.07}_{-0.09}$	$3.13^{+0.02+0.18}_{-0.02-0.18}$	–
	$\bar{B}_s \to \rho^0 K^{*0}$	$2.79^{+2.75}_{-1.97}$	$2.78^{+2.74\ +0.04}_{-1.96\ -0.06}$	$1.94^{+2.52}_{-0.10}$	–	–
	$\bar{B}_s \to \omega K^{*0}$	$2.72^{+2.85}_{-1.83}$	$2.73^{+2.83\ +0.04}_{-1.81\ -0.05}$	$2.18^{+0.33}_{-0.28}$	–	–
$\phi_\perp + \pi$	$\bar{B}_s \to \rho^- K^{*+}$	$3.16^{+0.22}_{-0.24}$	$3.20^{+0.22\ +0.23}_{-0.24\ -0.22}$	3.07 ± 0.08	–	–
	$\bar{B}_s \to \rho^0 K^{*0}$	$2.71^{+2.84}_{-1.87}$	$2.78^{+2.65\ +0.05}_{-1.96\ -0.10}$	$1.99^{+2.53}_{-0.10}$	–	–
	$\bar{B}_s \to \omega K^{*0}$	$2.65^{+2.89}_{-1.75}$	$2.70^{+2.79\ +0.04}_{-1.82\ -0.08}$	$2.23^{+0.32}_{-0.27}$	–	–
$\Delta\phi_\parallel$	$\bar{B}_s \to \rho^- K^{*+}$	$0.13^{+0.01}_{-0.01}$	$0.12^{+0.01\ +0.06}_{-0.01\ -0.13}$	$0.12^{+0.05}_{-0.05}$	$0.06^{+0.02+0.11}_{-0.02-0.12}$	–
	$\bar{B}_s \to \rho^0 K^{*0}$	$-0.40^{+0.72}_{-0.28}$	$-0.33^{+0.73\ +0.33}_{-0.25\ -0.12}$	$-0.32^{+2.74}_{-0.16}$	–	–
	$\bar{B}_s \to \omega K^{*0}$	$0.17^{+0.24}_{-0.61}$	$0.11^{+0.22\ +0.11}_{-0.61\ -0.34}$	$0.31^{+0.31}_{-0.24}$	–	–
$\Delta\phi_\perp$	$\bar{B}_s \to \rho^- K^{*+}$	$0.09^{+0.02}_{-0.02}$	$0.11^{+0.02\ +0.06}_{-0.02\ -0.14}$	$0.12^{+0.04}_{-0.05}$	–	–
	$\bar{B}_s \to \rho^0 K^{*0}$	$-0.41^{+0.85}_{-0.24}$	$-0.21^{+0.34\ +0.40}_{-0.30\ -0.14}$	$-0.36^{+2.22}_{-0.16}$	–	–
	$\bar{B}_s \to \omega K^{*0}$	$0.20^{+0.75}_{-0.74}$	$-0.05^{+0.33\ +0.13}_{-0.20\ -0.38}$	$0.36^{+0.31}_{-0.24}$	–	–

implies that the endpoint parameters are topology-dependent, and it therefore confirms the suggestion proposed in Refs. [23,24].

In this case, we obtain

$$\chi^2_{\rm min}/n_{\rm dof} = 11.2/7, \quad p\ \text{value} = 0.13 \tag{50}$$

at the best-fit point. The deviations of the theoretical results from data are summarized in the fifth column of Table 2. We again find that the observable $\mathcal{B}(\bar{B}_s \to \phi K^{*0})$ results in the large $\chi^2_{\rm min}$ and small p-value. Numerically, one can find $\chi^2_{\mathcal{B}(\bar{B}_s \to \phi K^{*0})}/\chi^2_{\rm min} = 90\%$, which is similar to case I. If we disregard $\mathcal{B}(\bar{B}_s \to \phi K^{*0})$, we can find

$$\chi^2_{\rm min}/n_{\rm dof} = 1.65/6, \quad p\ \text{value} = 0.95. \tag{51}$$

Comparing case II with case I, we find from Table 2 that their main difference is in the deviations for the observables of $\bar{B}_s \to K^{*0}\bar{K}^{*0}$ decay: $0.00\,\sigma$ vs. $+4.31\,\sigma$ for $\mathcal{B}$, $+0.13\,\sigma$ vs. $+5.99\,\sigma$ for f_L, and $-1.21\,\sigma$ vs. $-4.96\,\sigma$ for $f_\perp$, which again indicates that the abnormal data for $\bar{B}_s \to K^{*0}\bar{K}^{*0}$ decay can be explained through the WA contributions. However, in both cases I and II, the deviations for $\mathcal{B}(\bar{B}_s \to \phi K^{*0})$, $-2.57\,\sigma$ and $-3.17\,\sigma$, are very large; this implies that the measured large $\mathcal{B}(\bar{B}_s \to \phi K^{*0}) = (1.13 \pm 0.30) \times 10^{-6}$ [34], which is much larger than all

Table 5 Theoretical results for the $b \to s$ induced $\bar{B}_s \to K^{*-}K^{*+}$, $\rho^0\phi$ and $\omega\phi$ decays

Observable	Decay mode	Case I	Case II	pQCD [65]	QCDF [53]	QCDF [19]
$\mathcal{B}[10^{-6}]$	$\bar{B}_s \to K^{*-}K^{*+}$	$20.0^{+1.0}_{-1.0}$	$9.7^{+0.9+6.9}_{-0.6-5.4}$	$5.4^{+2.7+1.8+0.3}_{-1.7-1.4-0.5}$	$9.1^{+2.5+10.2}_{-2.2-5.9}$	$7.6^{+1.0+2.3}_{-1.0-1.8}$
	$\bar{B}_s \to \rho^0\phi$	$0.41^{+0.11}_{-0.09}$	$0.41^{+0.11+0}_{-0.09-0}$	$0.23^{+0.15+0.03+0.01}_{-0.05-0.01-0.02}$	$0.40^{+0.12+0.27}_{-0.10-0.04}$	$0.18^{+0.01+0.09}_{-0.01-0.04}$
	$\bar{B}_s \to \omega\phi$	$0.25^{+0.34}_{-0.15}$	$0.25^{+0.34+0}_{-0.15-0}$	$0.17^{+0.10+0.05+0.00}_{-0.07-0.04-0.01}$	$0.10^{+0.05+0.48}_{-0.03-0.12}$	$0.18^{+0.44+0.47}_{-0.12-0.04}$
$A_{CP}[\%]$	$\bar{B}_s \to K^{*-}K^{*+}$	$-34.4^{+4.3}_{-3.7}$	$20.7^{+5.8+8.4}_{-6.0-18.3}$	$8.8^{+2.5+0.5+0.0}_{-8.9-2.9-0.2}$	2^{+0+40}_{-0-15}	21^{+1+2}_{-2-4}
	$\bar{B}_s \to \rho^0\phi$	$24.5^{+25.1}_{-20.9}$	$24.5^{+25.1+0}_{-20.9-0}$	$-4.3^{+0.6+0.6+1.2}_{-0.5-0.5-1.0}$	19^{+5+56}_{-5-67}	83^{+1+10}_{-0-36}
	$\bar{B}_s \to \omega\phi$	$-14.5^{+18.9}_{-18.7}$	$-14.5^{+18.9+0}_{-18.7-0}$	$28.0^{+1.3+0.5+3.4}_{-3.2-2.3-5.1}$	8^{+3+102}_{-3-56}	-8^{+3+20}_{-1-15}
$A^0_{CP}[\%]$	$\bar{B}_s \to K^{*-}K^{*+}$	$-15.5^{+3.2}_{-2.9}$	$40.5^{+15.3+41.9}_{-13.6-37.3}$	$45.4^{+19.0}_{-23.4}$	11^{+3+7}_{-3-17}	–
	$\bar{B}_s \to \rho^0\phi$	$-4.5^{+24.6}_{-12.9}$	$-4.5^{+24.6+0}_{-12.9-0}$	$3.27^{+1.07}_{-1.19}$	11^{+4+10}_{-3-8}	–
	$\bar{B}_s \to \omega\phi$	$0.2^{+3.7}_{-2.5}$	$0.2^{+3.7+0}_{-2.5-0}$	$-2.24^{+6.67}_{-5.45}$	–	–
$A^{\perp}_{CP}[\%]$	$\bar{B}_s \to K^{*-}K^{*+}$	$37.1^{+4.4}_{-4.4}$	$-31.6^{+5.5+21.1}_{-5.3-12.8}$	$-32.9^{+5.6}_{-4.0}$	–	–
	$\bar{B}_s \to \rho^0\phi$	$71.7^{+16.3}_{-16.7}$	$71.7^{+16.3+0}_{-16.7-0}$	$-32.8^{+7.4}_{-5.8}$	–	–
	$\bar{B}_s \to \omega\phi$	$-1.0^{+11.4}_{-6.5}$	$-1.0^{+11.4+0}_{-6.5-0}$	$4.38^{+17.52}_{-15.93}$	–	–
$f_L[\%]$	$\bar{B}_s \to K^{*-}K^{*+}$	$64.4^{+1.2}_{-2.7}$	$33.9^{+4.7+9.9}_{-4.0-14.2}$	$42^{+13+3+5}_{-9-3-6}$	67^{+4+31}_{-5-26}	52^{+3+20}_{-5-21}
	$\bar{B}_s \to \rho^0\phi$	$93.8^{+1.6}_{-12.1}$	$93.8^{+1.6+0}_{-12.1-0}$	86^{+1+1+0}_{-1-1-0}	81^{+3+9}_{-4-12}	88^{+1+2}_{-0-18}
	$\bar{B}_s \to \omega\phi$	$55.1^{+32.7}_{-16.3}$	$55.1^{+32.7+0}_{-16.3-0}$	69^{+8+8+2}_{-9-9-2}	–	95^{+1+0}_{-2-42}
$f_\perp[\%]$	$\bar{B}_s \to K^{*-}K^{*+}$	$16.1^{+0.9}_{-0.8}$	$40.6^{+3.9+5.6}_{-3.6-12.9}$	$27.7^{+5.2}_{-7.0}$	–	–
	$\bar{B}_s \to \rho^0\phi$	$2.8^{+5.7}_{-0.8}$	$2.8^{+5.7+0}_{-0.8-0}$	$8.89^{+0.80}_{-1.06}$	–	–
	$\bar{B}_s \to \omega\phi$	$23.0^{+8.4}_{-16.9}$	$23.0^{+8.4+0}_{-16.9-0}$	$16.1^{+7.3}_{-5.8}$	–	–
$\phi_\parallel + \pi$	$\bar{B}_s \to K^{*-}K^{*+}$	$2.86^{+0.10}_{-0.09}$	$1.94^{+0.10+0.59}_{-0.11-0.54}$	$3.53^{+0.33}_{-0.25}$	$2.84^{+0.02+1.00}_{-0.03-0.61}$	–
	$\bar{B}_s \to \rho^0\phi$	$3.01^{+0.22}_{-0.33}$	$3.01^{+0.22+0}_{-0.33-0}$	$3.11^{+0.10}_{-0.09}$	$1.60^{+0.05+0.10}_{-0.06-0.15}$	–
	$\bar{B}_s \to \omega\phi$	$2.90^{+0.24}_{-0.30}$	$2.90^{+0.24+0}_{-0.30-0}$	$3.38^{+0.20}_{-0.17}$	$2.00^{+0+0.44}_{-0-0.87}$	–
$\phi_\perp + \pi$	$\bar{B}_s \to K^{*-}K^{*+}$	$2.76^{+0.10}_{-0.11}$	$1.78^{+0.13+0.13}_{-0.13-0.12}$	$3.54^{+0.36}_{-0.24}$	–	–
	$\bar{B}_s \to \rho^0\phi$	$2.95^{+0.31}_{-0.34}$	$2.95^{+0.31+0}_{-0.34-0}$	3.29 ± 0.09	–	–
	$\bar{B}_s \to \omega\phi$	$2.92^{+0.19}_{-0.14}$	$2.92^{+0.19+0}_{-0.14-0}$	$3.35^{+0.30}_{-0.23}$	–	–
$\Delta\phi_\parallel$	$\bar{B}_s \to K^{*-}K^{*+}$	$-0.11^{+0.04}_{-0.04}$	$0.49^{+0.14+0.43}_{-0.13-0.20}$	$0.94^{+0.11}_{-0.14}$	$-0.15^{+0.03+0.92}_{-0.03-0.17}$	–
	$\bar{B}_s \to \rho^0\phi$	$0.41^{+0.32}_{-0.19}$	$0.41^{+0.32+0}_{-0.19-0}$	-0.44 ± 0.10	$-0.13^{+0.03+0.17}_{-0.03-0.13}$	–
	$\bar{B}_s \to \omega\phi$	$0.24^{+0.17}_{-0.09}$	$0.24^{+0.17+0}_{-0.09-0}$	-0.37 ± 0.12	$0.11^{+0.03+0.70}_{-0.03-0.63}$	–
$\Delta\phi_\perp$	$\bar{B}_s \to K^{*-}K^{*+}$	$-0.01^{+0.03}_{-0.04}$	$0.50^{+0.09+0.37}_{-0.10-0.20}$	$0.93^{+0.11}_{-0.14}$	–	–
	$\bar{B}_s \to \rho^0\phi$	$0.51^{+0.34}_{-0.37}$	$0.51^{+0.34+0}_{-0.37-0}$	$-0.64^{+0.11}_{-0.10}$	–	–
	$\bar{B}_s \to \omega\phi$	$0.26^{+0.18}_{-0.10}$	$0.26^{+0.18+0}_{-0.10-0}$	$-0.33^{+0.16}_{-0.19}$	–	–

of current predictions, $\sim 0.4 \times 10^{-6}$, in pQCD [65] and QCDF [19,53], is hardly to be accommodated by the WA contributions due to the constraints from the other observables and decay modes.

3.5 Updated results of QCDF for charmless $B_s \to VV$ decays

Using the fitted results given by Eqs. (43), (44) (case I) and (48), (49) (case II) for $(\rho_A^{i,f}, \phi_A^{i,f})$, Eq. (42) for (ρ_H, ϕ_H), and the other input parameters listed in Table 1, we now present in Tables 3, 4, 5 and 6 our updated theoretical results (posterior predictions[5]) for the branching ratios, CP-asymmetries, polarization fractions and relative phases in $\bar{B}_s \to \rho K^*$, ωK^*, ϕK^*, $\bar{K}^* K^*$, $\phi\phi$, $\rho\phi$, $\omega\phi$, $\rho\rho$, $\rho\omega$, $\omega\omega$ decays, where the previous predictions in the QCDF [19,53] and pQCD [65] approaches are also listed for comparison. The first uncertainty for the results of cases I and II in these tables is caused by the input parameters listed in Table 1 and ϕ_H given by Eq. (42); the second uncertainty for the results of case II cor-

[5] Our updated theoretical results in Tables 3, 4, 5 and 6 should be treated as posterior predictions since they are based on current data and the model for the endpoint regularization of HSS and WA contributions in QCDF.

Table 6 Theoretical results for pure annihilation $\bar{B}_s \to \rho\rho$, $\rho\omega$ and $\omega\omega$ decays. Our results $A^0_{CP} = 0$, $\Delta\phi_\perp = 0$, $\Delta\phi_\parallel = 0$ are in agreement with previous ones and are, therefore, not listed here

Observable	Decay mode	Case I	Case II	pQCD [65]	QCDF [53]	QCDF [19]
$\mathcal{B}[10^{-6}]$	$\bar{B}_s \to \rho^+\rho^-$	$25.6^{+1.3}_{-1.3}$	$10.4^{+0.2+6.7}_{-0.3-4.9}$	$1.5^{+0.7+0.2+0.0}_{-0.6-0.2-0.1}$	$0.34^{+0.03+0.60}_{-0.03-0.38}$	$0.68^{+0.04+0.73}_{-0.04-0.53}$
	$\bar{B}_s \to \rho^0\rho^0$	$15.2^{+4.2}_{-3.8}$	$5.2^{+0.1+3.4}_{-0.1-2.5}$	$0.74^{+0.39+0.22+0.00}_{-0.24-0.14-0.00}$	$0.17^{+0.01+0.30}_{-0.01-0.19}$	$0.34^{+0.02+0.36}_{-0.02-0.26}$
	$\bar{B}_s \to \rho^0\omega$	$0.05^{+0.01}_{-0.01}$	$0.02^{+0.00+0.01}_{-0.00-0.01}$	$0.009^{+0.003+0.001+0.000}_{-0.003-0.002-0.001}$	< 0.01	$0.004^{+0.0+0.005}_{-0.0-0.003}$
	$\bar{B}_s \to \omega\omega$	$9.6^{+1.6}_{-1.4}$	$3.9^{+0.7+2.5}_{-0.6-1.9}$	$0.40^{+0.16+0.10+0.00}_{-0.18-0.10-0.01}$	$0.11^{+0.01+0.20}_{-0.01-0.12}$	$0.19^{+0.02+0.21}_{-0.02-0.15}$
$A_{CP}[\%]$	$\bar{B}_s \to \rho^+\rho^-$	0 ± 0	0 ± 0	$-2.9^{+0.7+1.5+0.2}_{-1.1-1.3-0.2}$	–	0
	$\bar{B}_s \to \rho^0\rho^0$	0 ± 0	0 ± 0	$-2.9^{+0.7+1.5+0.2}_{-1.1-1.3-0.2}$	–	0
	$\bar{B}_s \to \rho^0\omega$	0 ± 0	0 ± 0	$11.1^{+1.0+1.9+1.2}_{-1.5-4.4-1.4}$	–	0
	$\bar{B}_s \to \omega\omega$	0 ± 0	0 ± 0	$-3.3^{+0.8+1.5+0.5}_{-1.0-1.4-0.2}$	–	0
$A^\perp_{CP}[\%]$	$\bar{B}_s \to \rho^+\rho^-$	0 ± 0	0 ± 0	$30.5^{+15.0}_{-16.3}$	–	–
	$\bar{B}_s \to \rho^0\rho^0$	0 ± 0	0 ± 0	$30.5^{+15.0}_{-16.3}$	–	–
	$\bar{B}_s \to \rho^0\omega$	0 ± 0	0 ± 0	$27.9^{+9.3}_{-9.9}$	–	–
	$\bar{B}_s \to \omega\omega$	0 ± 0	0 ± 0	$30.8^{+14.0}_{-15.3}$	–	–
$f_L[\%]$	$\bar{B}_s \to \rho^+\rho^-$	83 ± 1	55^{+1+13}_{-1-9}	~ 100	–	~ 100
	$\bar{B}_s \to \rho^0\rho^0$	83 ± 1	55^{+1+13}_{-1-9}	~ 100	–	~ 100
	$\bar{B}_s \to \rho^0\omega$	83 ± 1	55^{+1+13}_{-1-9}	~ 100	–	~ 100
	$\bar{B}_s \to \omega\omega$	83 ± 2	54^{+1+13}_{-1-9}	~ 100	–	~ 100
$f_\perp[\%]$	$\bar{B}_s \to \rho^+\rho^-$	8 ± 1	25^{+0+5}_{-0-8}	~ 0.0	–	–
	$\bar{B}_s \to \rho^0\rho^0$	8 ± 1	25^{+0+5}_{-0-8}	~ 0.0	–	–
	$\bar{B}_s \to \rho^0\omega$	8 ± 1	25^{+1+5}_{-1-8}	~ 0.0	–	–
	$\bar{B}_s \to \omega\omega$	8 ± 1	25^{+1+5}_{-1-7}	~ 0.0	–	–
$\phi_\parallel + \pi$	$\bar{B}_s \to \rho^+\rho^-$	2.60 ± 0.20	$1.79^{+0.10+0.24}_{-0.10-0.22}$	3.40 ± 0.04	–	–
	$\bar{B}_s \to \rho^0\rho^0$	2.61 ± 0.31	$1.79^{+0.10+0.24}_{-0.10-0.22}$	3.40 ± 0.04	–	–
	$\bar{B}_s \to \rho^0\omega$	2.61 ± 0.30	$1.80^{+0.12+0.24}_{-0.12-0.22}$	3.48 ± 0.04	–	–
	$\bar{B}_s \to \omega\omega$	2.60 ± 0.50	$1.80^{+0.12+0.24}_{-0.12-0.22}$	3.40 ± 0.04	–	–
$\phi_\perp + \pi$	$\bar{B}_s \to \rho^+\rho^-$	2.59 ± 0.21	$1.68^{+0.10+0.23}_{-0.10-0.23}$	$3.27^{+0.16}_{-0.15}$	–	–
	$\bar{B}_s \to \rho^0\rho^0$	2.59 ± 0.32	$1.68^{+0.12+0.23}_{-0.12-0.23}$	$3.27^{+0.16}_{-0.15}$	–	–
	$\bar{B}_s \to \rho^0\omega$	2.59 ± 0.31	$1.68^{+0.10+0.23}_{-0.10-0.23}$	$2.63^{+0.18}_{-0.22}$	–	–
	$\bar{B}_s \to \omega\omega$	2.58 ± 0.50	$1.70^{+0.12+0.23}_{-0.12-0.23}$	$3.27^{+0.16}_{-0.11}$	–	–

responds to the uncertainties of $(\rho_A^{i,f}, \phi_A^{i,f})$ given by Eqs. (48) and (49).

One can find from these tables that most of our results for the observables are in agreement with the current experimental data including the abnormal $f_{L,\perp}(\bar{B}_s \to K^{*0}\bar{K}^{*0})$; the only exception is for $\mathcal{B}(\bar{B}_s \to \phi K^{*0})$. A detailed discussion has been presented in the last subsections. More theoretical and experimental efforts are needed to confirm or refute this possible puzzle.

Our results are also generally in consistence with the previous theoretical predictions in QCDF [19,53] and pQCD [65] within the theoretical uncertainties. The most obvious differences are the results for the pure annihilation B_s decays, which can be seen from Table 6. Our results for the branching ratios of $\bar{B}_s \to \rho\rho$, $\rho\omega$ and $\omega\omega$ decays are about one order larger than the previous predictions; moreover, our results, $f_{L,\perp} \sim 55, 25\%$, are also obviously different from $f_{L,\perp} \sim 100, 0\%$ [53,65]. These differences in fact can easily be understood from the following: (i) The best-fit value of ρ_A^i is very large in order to fit the abnormal $f_{L,\perp}(\bar{B}_s \to K^{*0}\bar{K}^{*0}) \sim 20, 58\%$ in case II as discussed above; it results in sizable nonfactorizable annihilation contributions. (ii) The pure annihilation decays, $\bar{B}_s \to \omega\phi$, $\rho\rho$, $\rho\omega$, $\omega\omega$, are only relevant to the nonfactorizable annihilation amplitudes. Therefore, it can be briefly concluded that, if one requires the WA corrections to account for the abnormal $f_{L,\perp}(\bar{B}_s \to K^{*0}\bar{K}^{*0})$ measured by the LHCb collaboration, the large branching ratios and transverse polarization fractions of $\bar{B}_s \to \rho\rho$, $\rho\omega$ and $\omega\omega$ decays will be expected accordingly. Interestingly, the large nonfactorizable annihila-

tion contributions have been observed in the pure annihilation $B_s \to \pi^+\pi^-$ decay [22–24,36–38].

Finally, we would like to point out that the allowed spaces for the endpoint parameters are still very large, especially in case I; our results are only based on the best-fit points, and the other allowed spaces for $(\rho_A^{i,f}, \phi_A^{i,f})$ shown in Figs. 2 and 4 are not taken into account here; moreover, it is also not clear whether the annihilation corrections should account for the abnormal $f_{L,\perp}(\bar{B}_s \to K^{*0}\bar{K}^{*0})$. More data on $B_s \to VV$ decays are needed for a definite conclusion. The pure annihilation decays mentioned above, except for $\bar{B}_s \to \rho\omega$, having branching ratios $\gtrsim \mathcal{O}(10^{-7})$, are in the scope of the LHCb and Belle-II experiments. Hence, a much clearer picture of the WA contributions in charmless $B_s \to VV$ decays is expected to be obtained from these dedicated heavy-flavor experiments in the near future.

4 Conclusion

In summary, we have studied the HSS and WA contributions in charmless $B_s \to VV$ decays. In order to probe their strength and possible strong phase, we have performed χ^2-analyses for the endpoint parameters under the constraint from the measured $\bar{B}_s \to \rho^0\phi$, ϕK^{*0}, $\phi\phi$ and $K^{*0}\bar{K}^{*0}$ decay. It is found that the endpoint parameters in the factorizable and nonfactorizable annihilation topologies are non-universal at 68% C.L. due to the constraint from $\bar{B}_s \to K^{*0}\bar{K}^{*0}$ decay; this further confirms the findings in the previous work. Moreover, the abnormal polarization fractions $f_{L,\perp}(\bar{B}_s \to K^{*0}\bar{K}^{*0}) = (20.1\pm7.0)\%$, $(58.4\pm8.5)\%$ measured by the LHCb collaboration can be reconciled through the weak annihilation corrections with a large ρ_A^i. However, the $\mathcal{B}(\bar{B}_s \to \phi K^{*0})$ exhibits a significant tension between the data and theoretical results, which dominates the contributions to $\chi^2_{\rm min}$ in the fits. Using the best-fit endpoint parameters, we have also updated the theoretical results for the charmless $B_s \to VV$ decays within the framework of QCDF. It is found that the large branching fractions and transverse polarization fractions for the pure annihilation decays are possible if we require the WA contributions to account for the abnormal $f_{L,\perp}(\bar{B}_s \to K^{*0}\bar{K}^{*0})$. Our results and findings will be further tested by the LHCb and Belle-II experiments in the near future.

Acknowledgements We thank Dr. Xingbo Yuan at NCTS for helpful discussions. The work is supported by the National Natural Science Foundation of China under contract Nos. 11475055, 11675061, 11435003 and U1632109. Q. Chang is also supported by the Foundation for the Author of National Excellent Doctoral Dissertation of P. R. China (Grant No. 201317), the Program for Science and Technology Innovation Talents in Universities of Henan Province (Grant No. 14HASTIT036), the Excellent Youth Foundation of HNNU and the CSC.

Funded by SCOAP[3].

References

1. M. Beneke, G. Buchalla, M. Neubert, C.T. Sachrajda, Phys. Rev. Lett. **83**, 1914 (1999)
2. M. Beneke, G. Buchalla, M. Neubert, C.T. Sachrajda, Nucl. Phys. B **591**, 313 (2000)
3. Y.Y. Keum, H.N. Li, A.I. Sanda, Phys. Lett. B **504**, 6 (2001)
4. Y.Y. Keum, H.N. Li, A.I. Sanda, Phys. Rev. D **63**, 054008 (2001)
5. C.W. Bauer, S. Fleming, D. Pirjol, I.W. Stewart, Phys. Rev. D **63**, 114020 (2001)
6. C.W. Bauer, D. Pirjol, I.W. Stewart, Phys. Rev. D **65**, 054022 (2002)
7. M. Beneke, A.P. Chapovsky, M. Diehl, T. Feldmann, Nucl. Phys. B **643**, 431 (2002)
8. M. Beneke, T. Feldmann, Phys. Lett. B **553**, 267 (2003)
9. M. Beneke, M. Neubert, Nucl. Phys. B **675**, 333 (2003)
10. J.F. Sun, G.H. Zhu, D.S. Du, Phys. Rev. D **68**, 054003 (2003)
11. C.M. Arnesen, I.Z. Rothstein, I.W. Stewart, Phys. Lett. B **647**, 405 (2007). Erratum: [Phys. Lett. B **653**, 450 (2007)]
12. Z.J. Xiao, W.F. Wang, Y.Y. Fan. Phys. Rev. D **85**, 094003 (2012)
13. A. Ali, G. Kramer, Y. Li, C.D. Lu, Y.L. Shen, W. Wang, Y.M. Wang, Phys. Rev. D **76**, 074018 (2007)
14. Q. Chang, X.W. Cui, L. Han, Y.D. Yang, Phys. Rev. D **86**, 054016 (2012)
15. Y. Li, W.L. Wang, D.S. Du, Z.H. Li, H.X. Xu, Eur. Phys. J. C **75**(7), 328 (2015)
16. H.W. Huang, C.D. Lu, T. Morii, Y.L. Shen, G. Song, J. Zhu, Phys. Rev. D **73**, 014011 (2006)
17. Y. Li, C.D. Lu, Z.J. Xiao, X.Q. Yu, Phys. Rev. D **70**, 034009 (2004)
18. Y.D. Yang, F. Su, G.R. Lu, H.J. Hao, Eur. Phys. J. C **44**, 243 (2005)
19. H.Y. Cheng, C.K. Chua, Phys. Rev. D **80**, 114026 (2009)
20. H.Y. Cheng, K.C. Yang, Phys. Rev. D **78**, 094001 (2008). Erratum: [Phys. Rev. D **79**, 039903 (2009)]
21. H.Y. Cheng, C.K. Chua, Phys. Rev. D **80**, 114008 (2009)
22. C. Bobeth, M. Gorbahn, S. Vickers, Eur. Phys. J. C **75**(7), 340 (2015)
23. G. Zhu, Phys. Lett. B **702**, 408 (2011)
24. K. Wang, G. Zhu, Phys. Rev. D **88**, 014043 (2013)
25. Q. Chang, J. Sun, Y. Yang, X. Li, Phys. Rev. D **90**(5), 054019 (2014)
26. Q. Chang, J. Sun, Y. Yang, X. Li, Phys. Lett. B **740**, 56 (2015)
27. J. Sun, Q. Chang, X. Hu, Y. Yang, Phys. Lett. B **743**, 444 (2015)
28. Q. Chang, X. Hu, J. Sun, Y. Yang, Phys. Rev. D **91**, 074026 (2015)
29. Q. Chang, X.N. Li, J.F. Sun, Y.L. Yang, J. Phys. G **43**, 105004 (2016)
30. H.Y. Cheng, C.W. Chiang, A.L. Kuo, Phys. Rev. D **91**, 014011 (2015)
31. G. Bell, M. Beneke, T. Huber, X.Q. Li, Phys. Lett. B **750**, 348 (2015)
32. R. Fleischer, S. Recksiegel, F. Schwab, Eur. Phys. J. C **51**, 55 (2007)
33. X. Liu, H.N. Li, Z.J. Xiao, Phys. Rev. D **93**(1), 014024 (2016)
34. Y. Amhis et al., Heavy Flavor Averaging Group, arXiv:1412.7515. Updated results and plots available at: http://www.slac.stanford.edu/xorg/hfag
35. C. Patrignani et al. [Particle Data Group], Chin. Phys. C **40**(10), 100001 (2016)

36. T. Aaltonen et al. [CDF Collaboration], Phys. Rev. Lett. **108**, 211803 (2012)
37. Y.-T. Duh et al. [Belle Collaboration], Phys. Rev. D **87**(30, 031103 (2013)
38. R. Aaij et al. [LHCb Collaboration], JHEP **1210**, 037 (2012)
39. R. Aaij et al. [LHCb Collaboration], Phys. Rev. Lett. **118**(8), 081801 (2017)
40. T. Gershon, M. Needham, Comptes Rendus Phys. **16**, 435 (2015)
41. R. Aaij et al. [LHCb Collaboration], Phys. Lett. B **694**, 209 (2010)
42. R. Aaij et al. [LHCb Collaboration], Eur. Phys. J. C **73**(4), 2373 (2013)
43. R. Aaij et al. [LHCb Collaboration], Int. J. Mod. Phys. A **30**(07), 1530022 (2015)
44. The LHCb Collaboration [LHCb Collaboration], CERN-LHCC-2011-001
45. T. Abe et al. [Belle-II Collaboration], arXiv:1011.0352
46. G. Buchalla, A.J. Buras, M.E. Lautenbacher, Rev. Mod. Phys. **68**, 1125 (1996)
47. A.J. Buras, arXiv:hep-ph/9806471
48. G.P. Lepage, S.J. Brodsky, Phys. Rev. D **22**, 2157 (1980)
49. M. Beneke, J. Rohrer, D. Yang, Phys. Rev. Lett. **96**, 141801 (2006)
50. T. Huber, S. Kränkl, X.Q. Li, JHEP **1609**, 112 (2016)
51. D. Du, D. Yang, G. Zhu, Phys. Lett. B **509**, 263 (2001)
52. D. Du, D. Yang, G. Zhu, Phys. Rev. D **64**, 014036 (2001)
53. M. Beneke, J. Rohrer, D. Yang, Nucl. Phys. B **774**, 64 (2007)
54. M. Beneke, T. Huber, X.Q. Li, Nucl. Phys. B **832**, 109 (2010)
55. Q. Chang, L.X. Chen, Y.Y. Zhang, J.F. Sun, Y.L. Yang, Eur. Phys. J. C **76**(10), 523 (2016)
56. M. Beneke, X.Q. Li, L. Vernazza, Eur. Phys. J. C **61**, 429 (2009)
57. R. Aaij et al. [LHCb Collaboration], Phys. Rev. D **95**(1), 012006 (2017)
58. J.G. Korner, G.R. Goldstein, Phys. Lett. **89B**, 105 (1979)
59. K. De Bruyn, R. Fleischer, R. Knegjens, P. Koppenburg, M. Merk, N. Tuning, Phys. Rev. D **86**, 014027 (2012)
60. I. Dunietz, R. Fleischer, U. Nierste, Phys. Rev. D **63**, 114015 (2001)
61. J. Charles et al. [CKMfitter Group Collaboration], Eur. Phys. J. C **41**, 1 (2005). Updated results and plots available at: http://ckmfitter.in2p3.fr
62. S. Aoki et al. [Flavour Lattice Averaging Group], Eur. Phys. J. C **77**(2), 112 (2017)
63. A. Bharucha, D.M. Straub, R. Zwicky, JHEP **1608**, 098 (2016)
64. M. Dimou, J. Lyon, R. Zwicky, Phys. Rev. D **87**(7), 074008 (2013)
65. Z.T. Zou, A. Ali, C.D. Lu, X. Liu, Y. Li, Phys. Rev. D **91**, 054033 (2015)
66. R. Aaij et al. [LHCb Collaboration], JHEP **1507**, 166 (2015)
67. A.L. Kagan, Phys. Lett. B **601**, 151 (2004)
68. B. Aubert et al. [BaBar Collaboration], Phys. Rev. Lett. **93**, 231804 (2004)
69. M. Ladisa, V. Laporta, G. Nardulli, P. Santorelli, Phys. Rev. D **70**, 114025 (2004)
70. W.S. Hou, M. Nagashima, arXiv:hep-ph/0408007
71. H.N. Li, Phys. Lett. B **622**, 63 (2005)
72. C.S. Kim, Y.D. Yang, arXiv:hep-ph/0412364
73. Q. Chang, X.Q. Li, Y.D. Yang, JHEP **0706**, 038 (2007)
74. X.Q. Li, G.R. Lu, Y.D. Yang, Phys. Rev. D **68**, 114015 (2003). Erratum: [Phys. Rev. D **71**, 019902 (2005)]
75. H.N. Li, S. Mishima, Phys. Rev. D **71**, 054025 (2005)